

Final Degree Project

Biochemistry and Molecular Biology

Specialization in Clinical and Forensic Biochemistry

**DEVELOPMENT AND OPTIMIZATION OF A
MINIMAL-VOLUME $^1\text{H-NMR}$ PROTOCOL FOR
LIPOPROTEIN QUANTIFICATION IN CLINICAL
AND RESEARCH CONTEXTS**

Yosra Zaanan Chaaouaoue

Directed by Dr. Ricardo Rodríguez Calvo and Dra. Carla Merino
Ruiz



UNIVERSITAT ROVIRA i VIRGILI

Tarragona, 2025

This Final Degree Project has been based on the results obtained in my external Internship at Biosfer Teslab under the supervision of Carla Merino Ruiz and Pol Torné Charlez.



INDEX

ABBREVIATURES:	4
1. ABSTRACT:	6
2. INTRODUCTION:	7
2.1. NMR as an analytical tool for quantifying lipoproteins:.....	11
2.2. Liposcale test: an innovative advanced lipoprotein quantification test based on 2D 1H NMR DOSY spectroscopy.....	13
2.3. Limitations and optimization of sample volume in NMR protocols:.....	15
3. HYPOTHESIS AND OBJECTIVES:	16
4. MATERIAL AND METHODS:	16
4.1. Study Type and Experimental Design:.....	16
4.2. Biological Samples:.....	18
4.7. Statistical Analysis:.....	22
5. RESULTS:	22
6. DISCUSSION:	37
7. CONCLUSIONS:	39
8. BIBLIOGRAPHY:	40
9. ANNEXES:	41
9.1. ANNEX 1:.....	41
9.2. ANNEX 2:.....	46
9.3. ANNEX 3:.....	50

ABREVIATURES:

¹H-NMR: Proton nuclear magnetic resonance

2D ¹H NMR DOSY spectroscopy: Two-dimensional proton nuclear magnetic resonance spectroscopy with diffusion-ordered spectroscopy.

BSA: Bovine Serum Albumin

CPMG: Carr-Purcell-Meiboom-Gill

D₂O: Deuterium Oxide

FID: Free Induction Decay

HDL: High Density Lipoprotein

HDL-C: High Density Lipoprotein Cholesterol

HDL-P: High Density Lipoprotein Particles

HDL-TG: High Density Lipoprotein Triglycerides

HDL-Z: High Density Lipoprotein Average Size

IDL: Intermediate-density Lipoprotein

IDL-C: Intermediate-density Lipoprotein Cholesterol

IDL-TG: Intermediate-density Lipoprotein Triglycerides

ILD-C: Intermediate-density Lipoprotein Cholesterol (parecido a IDL-C)

L-HDL-P: High Density Lipoprotein Large Particles

L-LDL-P: Low Density Lipoprotein Large Particles

L-VLDL-P: Very Low Density Lipoprotein Large Particles

LDL: Low Density Lipoprotein

LDL-C: Low Density Lipoprotein Cholesterol

LDL-P: Low Density Lipoprotein Particles

LDL-TG: Low Density Lipoprotein Triglycerides

LDL-Z: Low Density Lipoprotein Average Size

LED: Longitudinal Eddy Delay

M-HDL-P: High Density Lipoprotein Medium Particles

M-LDL-P: Low Density Lipoprotein Medium Particles

M-VLDL-P: Very Low Density Lipoprotein Medium Particles

NMR: Nuclear Magnetic Resonance

NOESY: Nuclear Overhauser Effect Spectroscopy

PBS: Phosphate-Buffered Saline

r: Correlation Coefficient

S-HDL-P: High Density Lipoprotein Small Particles

S-LDL-P: Low Density Lipoprotein Small Particles

S-VLDL-P: Very Low Density Lipoprotein Small Particles

VLDL: Very Low Density Lipoprotein

VLDL-C: Very Low Density Lipoprotein Cholesterol

VLDL-P: Very Low Density Lipoprotein Particles

VLDL-TG: Very Low Density Lipoprotein Triglycerides

VLDL-Z: Very Low Density Lipoprotein Average Size

WHO: World Health Organization

1. ABSTRACT:

Introduction: Lipoproteins are essential for lipid transport in blood, and their profile is closely linked to cardiovascular risk. The Liposcale test enables a more advanced characterization of lipid profiles, but the current protocol used for this determination has volume limitations.

Objectives: Develop and validate a modified protocol that maintains the quality of lipoprotein profiling while working with reduced sample volumes.

Methodology: Nine serum samples were analyzed and classified by lipid concentration to assess the precision, reproducibility, and agreement of the proposed protocol in comparison to the original, using statistical analyses such as the Wilcoxon test, Bland-Altman plots, and Z-score transformations.

Results: The results obtained in this study suggest that it is possible to use the optimized protocol for reduced-volume samples, although there are some limitations.

Conclusions: The study demonstrates that it is possible to optimize a lipoprotein quantification protocol without compromising analytical accuracy, although certain limitations exist. Validation in a larger and more diverse cohort is recommended due to the limited sample size.

Keywords: RMN, Lipoproteins, Liposcale, Cardiovascular Diseases, Optimized Protocol, Reduced Volumes.

2. INTRODUCTION:

Due to the hydrophobic nature of certain lipids such as triglycerides and cholesterol, macromolecular complexes are required to transport them through the blood plasma. These molecules are known as lipoproteins and are composed of a central apolar core containing cholesterol esters and triglycerides, which is surrounded by a polar layer of phospholipids along with free cholesterol and apolipoproteins. The last ones facilitate the formation and function of lipoproteins, enabling them to be soluble in plasma. Figure 1 shows the schematic structure of a lipoprotein [1].

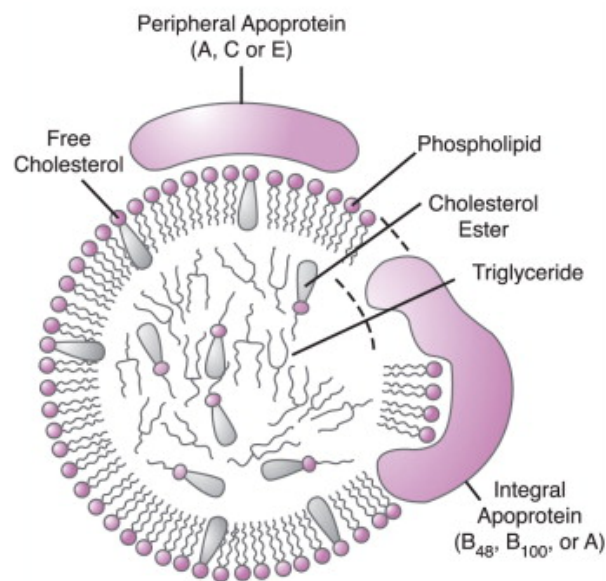


Figure 1. Schematic structure of a lipoprotein. Source: Morris, G. A. (2017). *Diffusion-Ordered Spectroscopy (DOSY)*, in *Encyclopedia of Spectroscopy and Spectrometry*, 3rd ed. Academic Press. © Elsevier.

Plasma lipoproteins can be classified into seven different categories based on their size, lipid composition, and apolipoproteins [1]. Each category has its specific function:

- **Chylomicrons** are responsible for transporting dietary lipids from the intestine to the tissues.
- **Very Low Density Lipoprotein (VLDL)** carries triglycerides synthesized in the liver to peripheral tissues.
- **Intermediate-density lipoprotein (IDL)** transport cholesterol from the liver to the cells and, subsequently, through its transformation, form LDL.
- **Low Density Lipoprotein (LDL)** delivers a large portion of plasma cholesterol to extrahepatic tissues.

- **High Density Lipoprotein (HDL)** is responsible for reverse cholesterol transport, meaning it collects excess cholesterol from tissues and redirects it to the liver for excretion.

Table 1 and Figure 2 provide a more detailed comparison of the lipoprotein classes, listing their typical density and size ranges, predominant lipid types, and characteristic apolipoproteins.

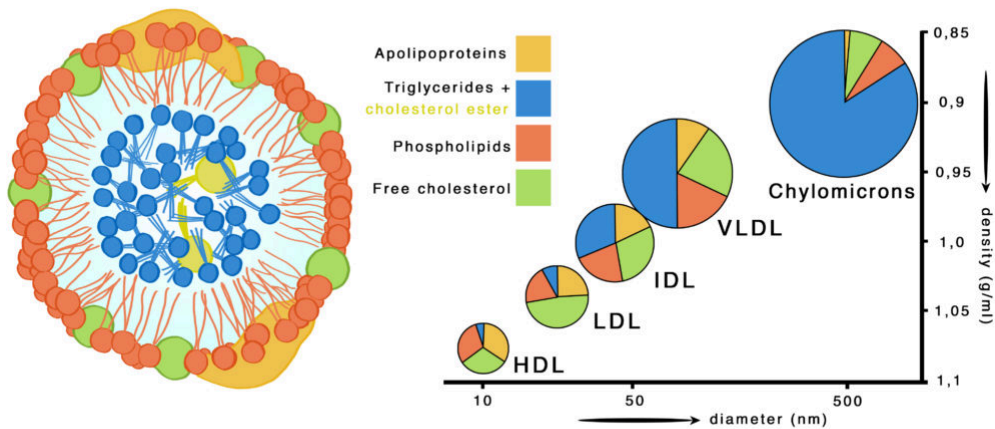


Figure 2. Classification of the different categories of lipoproteins based on their density and size. Adapted from “Lipoproteins”. Copyright 2023 by Biosfer Teslab.

Table 1. Classification of the different lipoproteins based on their density, size and composition.

Lipoprotein	Density (g/ml)	Size (nm)	Major Lipids	Major Apoproteins
Chylomicrons	<0.930	75-1200	Triglycerides	Apo B-48, Apo C, Apo E, Apo A-I, A-II, A-IV
Chylomicron Remnants	0.930- 1.006	30-80	Triglycerides Cholesterol	Apo B-48, Apo E
VLDL	0.930- 1.006	30-80	Triglycerides	Apo B-100, Apo E, Apo C
IDL	1.006- 1.019	25-35	Triglycerides Cholesterol	Apo B-100, Apo E, Apo C
LDL	1.019- 1.063	18- 25	Cholesterol	Apo B-100
HDL	1.063- 1.210	5- 12	Cholesterol Phospholipids	Apo A-I, Apo A-II, Apo C, Apo E

Lipoprotein	Density (g/ml)	Size (nm)	Major Lipids	Major Apoproteins
Lp (a)	1.055- 1.085	~30	Cholesterol	Apo B-100, Apo (a)

Plasma lipoproteins are closely associated with cardiovascular diseases, and this relationship is of critical importance. High levels of LDL particles in blood promote the accumulation of cholesterol in the arterial walls. This occurs because LDL particles can easily cross the endothelium and trigger the cascade of events involved in atherogenesis, eventually leading to the formation of atherosclerotic plaques. Thus, individuals with elevated LDL levels, and therefore a higher risk of developing atherosclerosis, are more prone to conditions such as myocardial infarction or cerebrovascular accidents. In contrast, high HDL levels are associated with a reduced risk of developing these pathologies [2].

Progression of Atherosclerosis

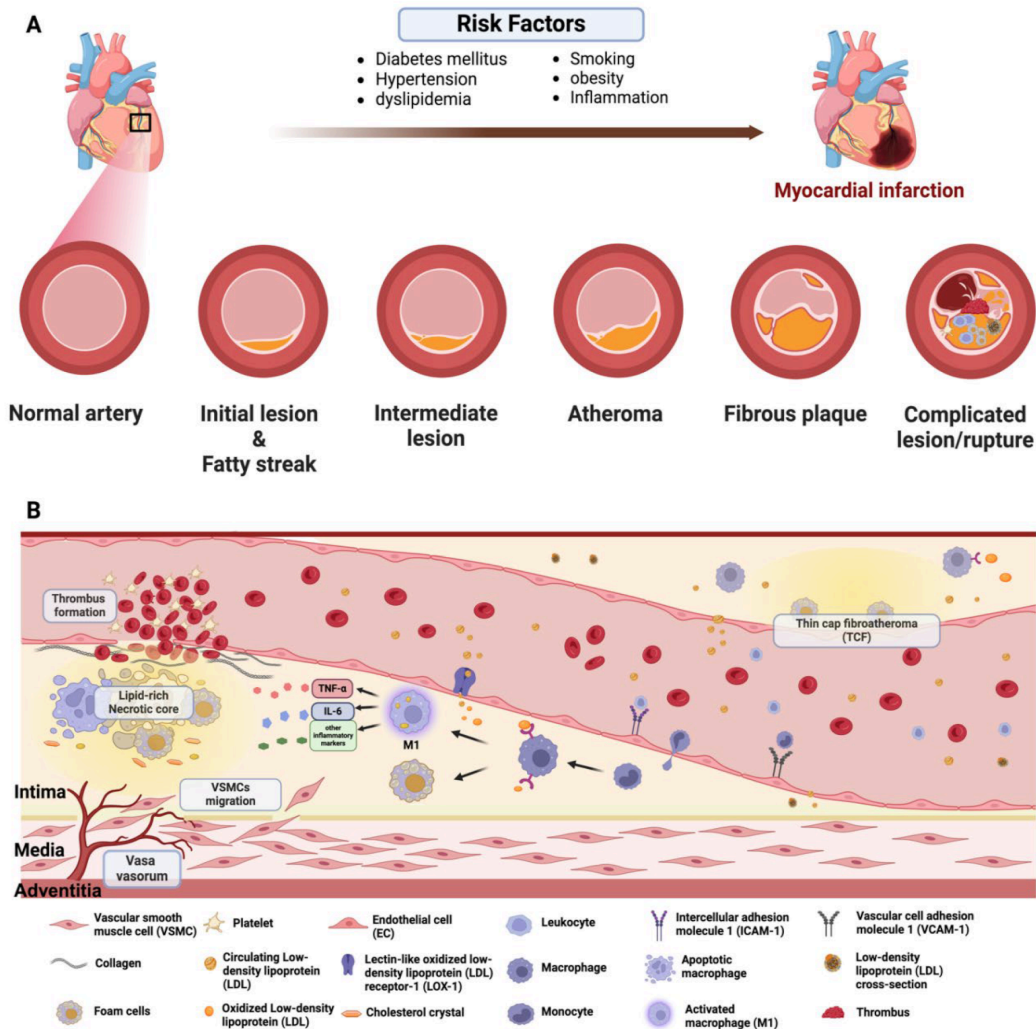


Figure 3. Pathophysiology of atherosclerosis. Reproduced from Alradwan et al. (2024), with permission from MDPI.

Cardiovascular diseases are currently the leading cause of death worldwide, according to the World Health Organization (WHO). It is estimated that approximately 17 million people die annually from these conditions, which account for 30% of all global deaths. Given this high prevalence, it is crucial to conduct a precise characterization of lipoprotein profiles, as they play a fundamental role in the development and progression of these diseases [3].

The accurate quantification of the different categories of lipoproteins is fundamental both for conducting a thorough assessment of the risk of developing cardiovascular disease and for effectively monitoring the response to treatment. In this context, nuclear magnetic resonance (NMR) has established itself as a promising tool for performing advanced characterizations of patients' lipoprotein profiles. This technology has not only proven to be fast, reproducible, and

robust, but with the proper subsequent methods, it also allows for the estimation of the average size, concentration, and distribution of plasma lipoproteins as done by Biosfer Teslab [4].

Unlike other methods such as ultracentrifugation or electrophoresis, which provide conventional lipoprotein profiles that are less accurate for predicting cardiovascular risk, this technique provides a more comprehensive and clinically relevant lipid profile [5].

2.1. NMR as an analytical tool for quantifying lipoproteins:

Nuclear magnetic resonance is an advanced spectroscopic method that makes use of the interaction of atomic nuclei possessing a magnetic moment with an external magnetic field. When a sample is placed in a strong magnetic field, in the case of proton nuclear magnetic resonance (¹H-NMR), hydrogen nuclei will align either with the magnetic field or against it. By prodding them with a witty radiofrequency pulse, they will be excited from their individual energy state to a higher energy state. After the radiofrequency pulse is turned off and they relax back to their original or basal state, they will emit energy in the form of a detectable signal [6].

The signal that is emitted is called the free induction decay (FID), and although at the initial acquisition state it is difficult to extract anything from it, it contains all the important information about the chemical environment of the nuclei. Since the rate at which each nucleus absorbs and emits energy is dependent upon the nuclei's electronic environment, the NMR signal provides structural and quantitative information about molecules that are contained in the sample [6].

When the FID signal is captured, the data is presented as a time-domain waveform, and cannot be interpreted directly. Thus, information contained in the time signal is mathematically transformed into the frequency domain, by a mathematical process known as Fourier Transform. By performing this transformation to the frequency domain, the resulting peaks seen in the NMR spectrum correspond to the different frequencies that designate the various chemical environments in the sample. The position (chemical shift) and intensity of the peaks (measure of amounts of detected nuclei in sample), and splitting pattern of the peaks (spin interactions), provide chemists with information to construct the structure, quantity and physical interaction of the molecules of interest [6].

When performing analysis using NMR, it is crucial to consider the choice of pulse sequence. The fluids being analyzed contain a wide range of low molecular weight metabolites, as well as

macromolecules such as lipoproteins, and the configuration of the pulse sequence allows for a size-filtering of the molecules that will be present in the spectra. Therefore, depending on the type of information one seeks to obtain, a specific pulse sequence should be selected. The most commonly used sequences in this context are:

- **Nuclear Overhauser Effect Spectroscopy (NOESY):** It is generally used to obtain general metabolic spectra, providing good resolution while preserving both metabolite signals and lipoprotein signals. It has the ability to show both kinds of molecules, the large ones and the small ones[6].
- **Longitudinal Eddy Delay (LED):** This sequence allows the separation of moving components of macromolecules through the modulation of the diffusion gradient. It is commonly used for molecular dynamics studies. Generally, it is the type of sequence used for lipoprotein studies due to its ability to analyze both molecular dynamics and relaxation of these macromolecules. It has the ability to filter small molecules, leaving only the large ones visible [6].
- **Carr-Purcell-Meiboom-Gill (CPMG):** This sequence is mainly used to obtain information on the transverse relaxation (T_2) of molecules in solution. It is useful for highlighting the signals of low molecular weight compounds that have short relaxation times. It has the capacity to filter large molecules, leaving only the small ones visible [6].

When biofluids such as serum or blood plasma are analyzed, the signals generated by $^1\text{H-NMR}$ correspond to the protons of the lipids present in the lipoproteins. These protons are primarily located in the methyl ($-\text{CH}_3$) and methylene ($-\text{CH}_2-$) groups of the lipid portion of the lipoproteins. The spectral signal from these regions (approximately 0.8-1.5 ppm) contains relevant information about the type, size, and number of lipoproteins present in the analyzed sample [4].

Each of the lipoprotein categories generates a distinct signal in the spectrum due to differences in molecular mobility and their lipid chemical environment. It is possible through techniques like prediction models based on experimental references, mathematical equations, or deconvolution processes (process of mathematically separating overlapping spectral signals to resolve individual components and accurately determine their chemical shifts and intensities), to quantitatively determine the concentration and mean size of these macromolecular complexes, as it's done by Biosfer Teslab through the Liposcale® test, which allows for the generation of an advanced lipoprotein profile [4].

2.2. Liposcale test: an innovative advanced lipoprotein quantification test based on 2D 1H NMR DOSY spectroscopy.

The Liposcale test is an innovative advanced technique developed by Biosfer Teslab, based on NMR spectroscopy, that enables the detailed characterization of the lipoprotein profile in serum or plasma samples. This test offers an alternative to traditional lipid quantification methods, as it provides information on the number, size, and concentration of the main lipoprotein subclasses.

Unlike conventional lipid profiles that only measure global parameters such as total cholesterol, LDL-C, HDL-C, and triglycerides, Liposcale allows the generation of a more quantitative and functionally representative lipoprotein profile for cardiovascular risk. Specifically, the Liposcale test provides information on the following parameters:

- a. **Estimated lipid concentration of triglycerides and cholesterol in each type of lipoprotein:** This information is obtained through prediction models based on experimental references [7].

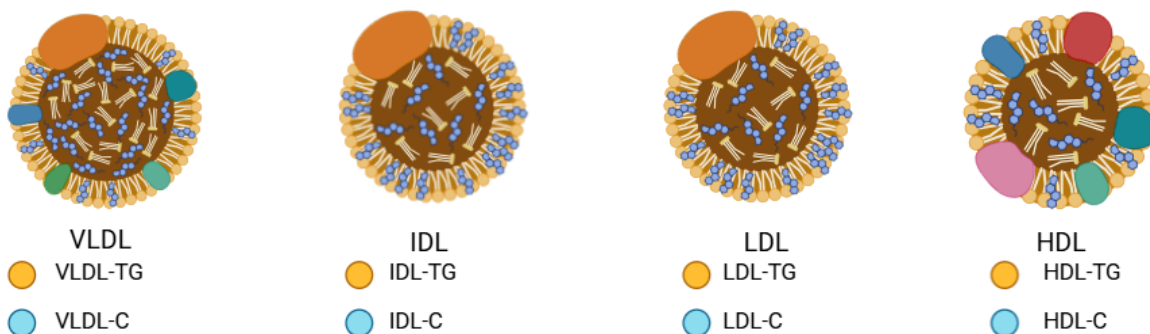


Figure 4. Classification of the different types of lipoproteins. Generated by BioRender.

- b. **Number of particles for each lipoprotein category and its subcategories:** The following parameter is derived from the analysis of the spectral region corresponding to methyl group resonances, where signals associated with lipoproteins are located [4]. Due to the partial overlap of these signals, mathematical modeling is used to separate them into individual components, following Biosfer Teslab in-house protocols and know-how.

This approach enables the estimation of contributions from different lipoprotein types and subtypes based on their spectral characteristics. The position, width, and area of these components reflect particle size and concentration, as the resonance frequencies of lipid methyl groups vary slightly with particle size.

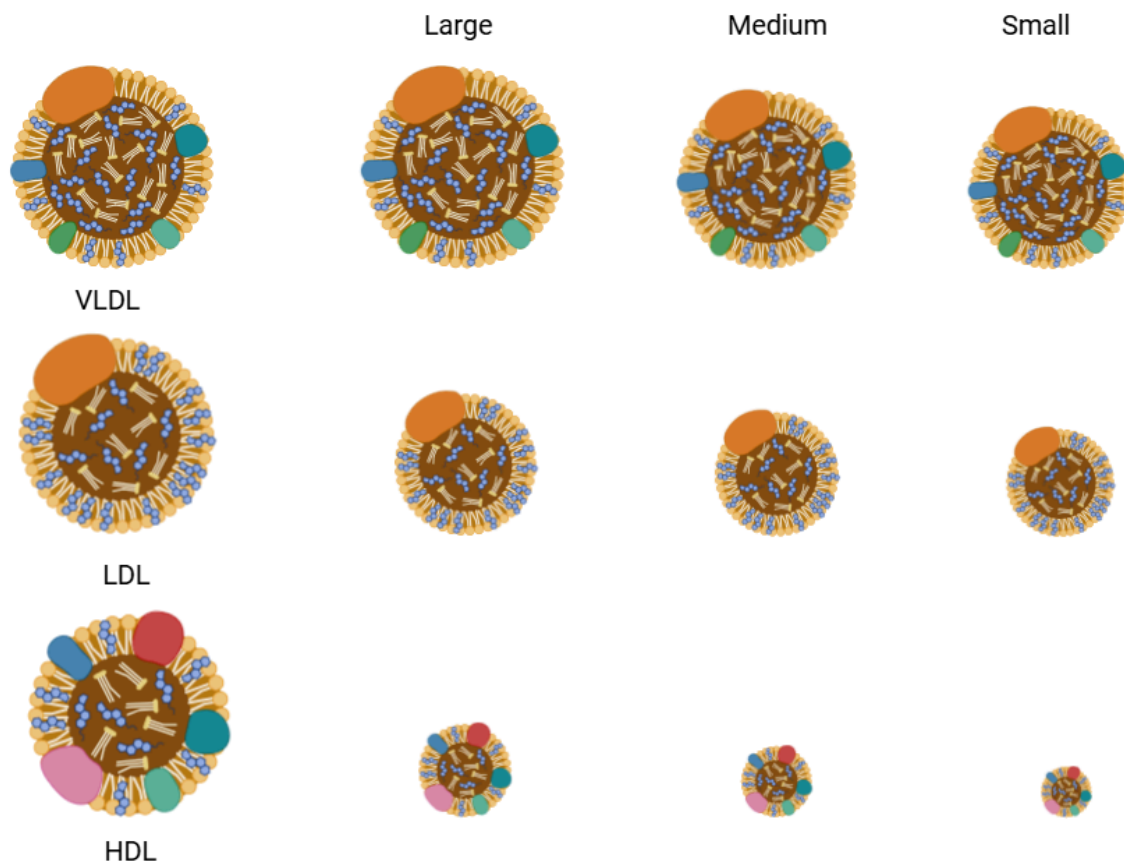


Figure 5. Classification of the different types of lipoproteins and their corresponding subcategories. Generated by BioRender.

- c. Average particle size of VLDL, LDL, and HDL:** Once the software has quantified the number of particles in each subclass and knows their characteristic diameter, that's obtained from experimental data, the average size is calculated, again, by Biosfer Teslab in-house methods [4].

This parameter is particularly relevant, especially for LDL, as it has relevant clinical value. As expressed above, profiles with small, dense LDL particles are more atherogenic than larger ones; therefore, a low average LDL size may indicate a higher-risk lipid profile.

- d. Relative distribution of particles by size:** This represents the percentage that each subclass occupies in relation to the total number of particles within that class. It allows for the identification of higher-risk lipid profiles. For example, a profile dominated by small, dense LDL particles may be indicative of atherogenicity.

$$\text{Relative distribution (\%)} = \frac{\text{Area corresponding to lipoprotein subclass}}{\text{Total area of all lipoprotein subclasses within the same group}} \times 100$$

The main advantage of this test lies in its ability to detect atherogenic lipid profiles that cannot be identified through conventional techniques. Liposcale represents a highly valuable tool in the advanced analysis of lipoprotein profiles, as it enables detailed and quantitative characterization of lipid particles using NMR. It provides a more accurate and functional view of cardiovascular risk and not only improves atherogenic risk stratification, but is also particularly useful in therapeutic monitoring and clinical studies where a deeper metabolic assessment is required [8].

2.3. Limitations and optimization of sample volume in NMR protocols:

The standard protocol employed for the Liposcale test consists of an initial sample volume of 200 μL , to which 300 μL of phosphate-buffered saline (PBS) and 50 μL of deuterated water are carefully added. This preparation ensures the proper environment for the NMR analysis, optimizing the spectral quality and enabling accurate characterization of lipoprotein profiles.

In many clinical and research contexts, the amount of available biological samples can often be limited. This scenario frequently occurs in pediatric research, in patients with life-threatening illnesses, or in projects that require several analyses to be carried out from a single extraction. It becomes crucial in these situations to have a process that enables accurate and repeatable results from smaller sample amounts. Additionally, minimizing the sample volume not only increases the analytical process's efficiency but also lowers expenses, decreases resource waste, and increases the technique's applicability in previously impractical circumstances.

To address the disadvantages outlined above, this project focuses on developing a new protocol that optimizes the existing one, specifically adapted for low-volume samples. It consists of an initial sample of 50 μL , to which 150 microliters of a 40 mg/mL or 30 mg/mL albumin solution are added. Albumin is used in this context primarily to stabilize the lipoprotein particles and maintain the viscosity of the sample, which facilitates its handling and analysis. Viscosity is a parameter that affects the acquisition of NMR spectra, so it is important to maintain the same viscosity as the original sample. Furthermore, albumin possesses characteristics that help keep the lipoprotein particles scattered throughout the solution by preventing lipoprotein aggregation and lowering the possibility of undesirable molecular interactions. To preserve the sample's pH and stability, 300 microliters of PBS are next added. Finally, 50 microliters of deuterated water are added to maximize the conditions for NMR spectroscopy.

One of the challenges when working with small sample volumes is that, for NMR analysis, it is necessary to reach a minimum total volume that properly fills the NMR tube and ensures correct magnetic field homogeneity. The minimum required volume depends on the probe and the NMR tube; in our case, the total sample volume for the probe used and 5 mm tubes is 550 μL . Therefore, it is not possible to simply scale everything down proportionally to 50 μL of starting sample. To address this, an albumin solution has been used to reach the required minimum volume, at a concentration that best simulates the physical conditions of the original sample.

3. HYPOTHESIS AND OBJECTIVES:

Hypothesis: It is possible to optimize the described standard lipoprotein quantification protocol using NMR to obtain reliable and reproducible results with significantly reduced sample volumes, without compromising analytical precision.

Main Objective: Develop and validate a modified protocol that maintains the quality of lipoprotein profiling while working with reduced sample volumes.

Specific Objectives:

1. Compare results obtained from both protocols.
2. Optimize the resolution of the results by varying the albumin concentration.

4. MATERIAL AND METHODS:

4.1. Study Type and Experimental Design:

This work presents an experimental study aimed at optimizing a lipoprotein quantification protocol using NMR spectroscopy with reduced sample volumes. To achieve this, a comparison was made between the standard protocol and the modified version designed for the study. Both protocols were applied to the same set of samples in order to assess the reliability, accuracy, and reproducibility of the results.

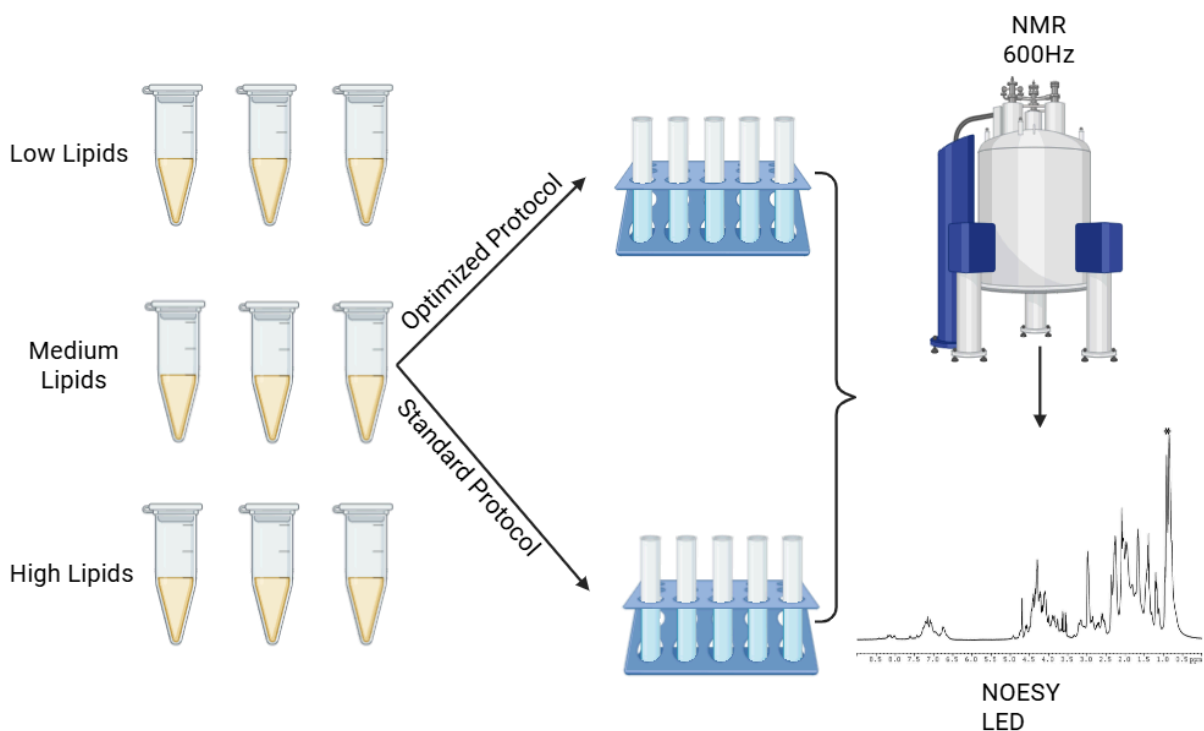


Figure 6. Schematic diagram of the methodology employed. Generated by Biorender.

A total of nine serum samples were processed and categorized into three distinct groups according to their lipid concentration (low, medium, and high) as it is shown in Table 2. This stratification allowed for the evaluation of the protocol's performance across a representative range of lipoprotein profiles, ensuring the robustness of the analysis under varying biological conditions.

Table 2. Classification of the samples into three distinct groups according to their lipid concentration.

Group	N	[Cholesterol] (mg/mL)	[Triglycerides] (mg/mL)
Low Lipid	3	<200	<150
Med Lipid	3	200-250	150-200
High Lipid	3	250-300	200-300

4.2. Biological Samples:

Nine human serum samples were used, previously stored at -80°C under stable conditions to prevent lipid degradation, as these are thermolabile samples. The samples were obtained from the clinical sample repository analyzed by Biosfer Teslab. Prior to analysis, all samples were thawed at room temperature and carefully homogenized to ensure comparability between replicates.

4.3. Reagents and Materials:

The following solutions and materials were used for the preparation of the samples included in the dilution/volume-scaling protocol:

- **Phosphate-buffered saline (PBS) and deuterium oxide (D_2O) (Eurisotop, France):** PBS was used to maintain a stable pH throughout the analysis, while D_2O provided the necessary deuterium signal for the water suppression and locking system during NMR acquisition.
- **Bovine serum albumin (BSA) at 40 mg/mL (Sigma-Aldrich, Spain):** BSA was added due to its capacity to stabilize lipoprotein particles and to mimic the natural viscosity of serum or plasma. This concentration was selected based on its widespread use in previous studies involving NMR-based lipoprotein quantification [9].
- **Bovine serum albumin (BSA) at 30 mg/mL (Sigma-Aldrich, Spain).**
- **Distilled water:** Used for the preparation and dilution of reagents as needed.

- **NMR tubes (DeuteroGmbH, Germany):** Specially designed NMR tubes suitable for high-resolution spectroscopy were used to ensure sample integrity and consistent spectral quality (5 mm).

4.4. Sample Preparation:

Each sample was processed identically according to its assigned protocol. In the standard protocol, as it is shown in Figure 7, 200 μL of sample were mixed with 300 μL of PBS and 50 μL of D_2O . In the optimized protocol, 50 μL of sample were combined with 150 μL of BSA solution (30 mg/mL or 40 mg/mL), 300 μL of PBS, and 50 μL of D_2O . Figure 8 provides a schematic explanation of the procedure.

All samples were prepared using a Gilson pipetting system, ensuring precise and homogeneous distribution of all reagents. The use of an automated pipetting system minimized handling variability and guaranteed both accuracy and reproducibility in the pipetted volumes, thereby reducing potential sources of error between replicates and across protocols.

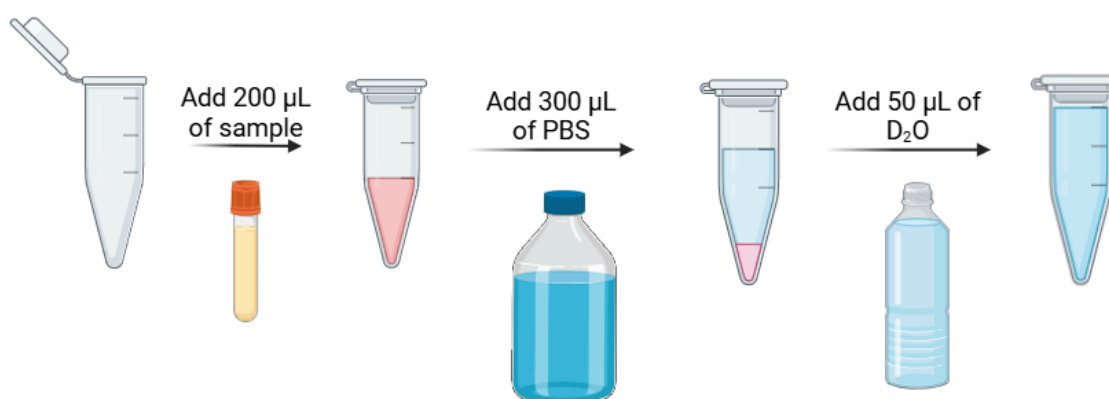


Figure 7. Standard protocol employed for the Liposcale test. Generated by BioRender.

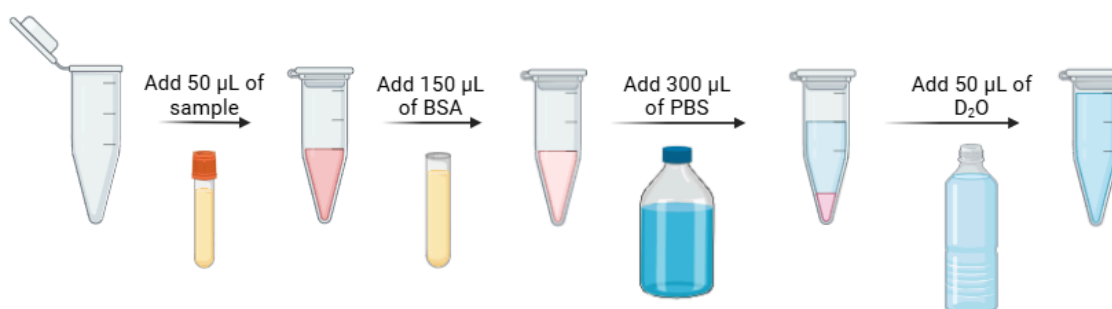


Figure 8. Optimized protocol employed for the Liposcale test. Generated by BioRender.

A 5 mL solution of BSA at a concentration of 40 mg/mL was prepared in advance for use in the optimized protocol, as it is shown in Figure 9. To prepare this solution, 200 mg of bovine serum albumin (BSA) were dissolved in 5 mL of MilliQ water. The mixture was transferred to a Falcon tube and gently agitated on an orbital shaker for 10 minutes to ensure complete dissolution and homogenization.



Figure 9. Methodology employed for the preparation of albumin 40 mg/mL. Generated by BioRender.

A new solution of albumin at a concentration of 30 mg/mL was also made from the original stock solution of 40 mg/mL, as it is shown in Figure 10. This adjustment of concentration was carried out with the intention of finding out how various concentrations of albumin could impact or improve the resolution of the experimental findings, potentially enhancing the sensitivity and accuracy of the analysis. A volume of 1.5 mL from the 40 mg/mL BSA (Bovine Serum Albumin) solution was mixed with 0.5 mL of Milli-Q water. The mixture was thoroughly homogenized to ensure uniform dilution, resulting in a final BSA concentration of 30 mg/mL.

In order to prepare the PBS (phosphate buffer solution) at 50 mM and pH 7.4, 2200 mg of disodium phosphate (Na_2HPO_4) and 1200 mg of monosodium phosphate (NaH_2PO_4) are weighed and dissolved in 350 mL of Milli-Q water under constant stirring. The pH is gradually adjusted to 7.1 by slowly adding 2 M NaOH using a micropipette. Then, 90 mL of deuterium oxide (D_2O) is added, and the pH is further adjusted drop by drop with 2 M NaOH until it reaches approximately 7.3. The total volume is then brought up to 500 mL with Milli-Q water. Finally, the pH is fine-tuned to exactly 7.4 if needed, and the solution is transferred to a properly labeled container indicating concentration, pH, and preparation date.

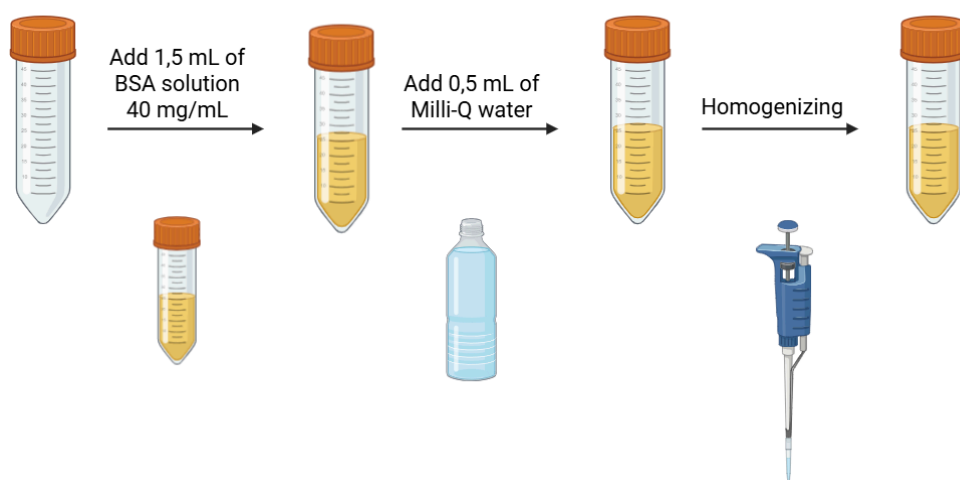


Figure 10. Methodology employed for the preparation of albumin 30 mg/mL. Generated by BioRender.

The optimized technique was performed in duplicate: once using the 40 mg/mL albumin solution and once using the 30 mg/mL solution. These were directly compared to the standard technique to ascertain if there were any differences in performance or resolution. All tests were performed under the same conditions and using the same samples to ensure consistency and allow reliable comparison of results. In summary, two parallel experiments were conducted. On one hand, a set of 9 samples was analyzed using the standard protocol and the optimized protocol with 40 mg/mL BSA. On the other hand, the same set of samples was analyzed using the optimized protocol with 30 mg/mL BSA. This approach allowed for a direct comparison of both optimized conditions against the standard method, under consistent experimental conditions.

4.5. Experimental Conditions for NMR Analysis:

Proton nuclear magnetic resonance spectra were recorded using 4 scans for NOESY, and 32 scans for LED, a constant temperature of 305.95 K and a gas flow rate of 400 L/h was maintained.

4.6. Spectral Processing and Analysis:

The acquired LED spectra were processed, as they are the most suitable for quantifying lipoproteins, using Liposcale software, which enabled the extraction of the following parameters: triglyceride and cholesterol concentrations by subclass, particle number (nmol/L), mean particle size, and the relative distribution of lipoprotein subclasses (VLDL, LDL, HDL), as described in section 2.2.

4.7. Statistical Analysis:

Regarding the statistical analysis section, various tests were conducted in order to assess the degree of similarity between the results obtained with the different protocols and their possible correlation. To this end, a univariate comparison was carried out. Significance was assessed through the **Wilcoxon** test since most of the results did not follow a normal distribution. Results are presented in Table 12 (Annex 2), and also through the following techniques:

- **Boxplots:** Based on the results obtained, these were represented as boxplots to visually depict the data distribution. This allowed for the identification of possible outliers and a general comparison of the different methods tested.
- **Bland-Altman:** This method was used to evaluate the level of agreement between the different protocols analyzed. This technique enables a graphical representation of the differences between protocols against their mean.

Subsequently, **Z-score** transformations were applied in order to normalize the values of the proposed protocols to the standard one, thus allowing the use of a common scale for comparisons. Once the values were normalized, they were again represented using Boxplots and Bland-Altman plots. The z-score transformation is a normalization method that centers the data around a mean of 0 and scales it to have a standard deviation of 1. This standardized data can then be rescaled to any desired mean and standard deviation, enabling comparison across different datasets.

All statistical analyses were performed using **R-4.3.1 software**, considering $p < 0.05$ as the threshold for statistical significance. The results were processed based on the data obtained after normalization using the Z-score method. The results obtained from the statistical analysis prior to Z-score normalization are included in Annex 2.

5. RESULTS:

It is worth noting that before running the Liposcale software to obtain the corresponding data for each of the parameters studied in the Liposcale test, a preprocessing step was carried out. This step consisted of aligning the baselines of the spectra obtained from the different protocols. This preliminary step was performed to ensure that the observed differences are due to the protocol itself and not the result of background noise, as can be observed in Figure 11.

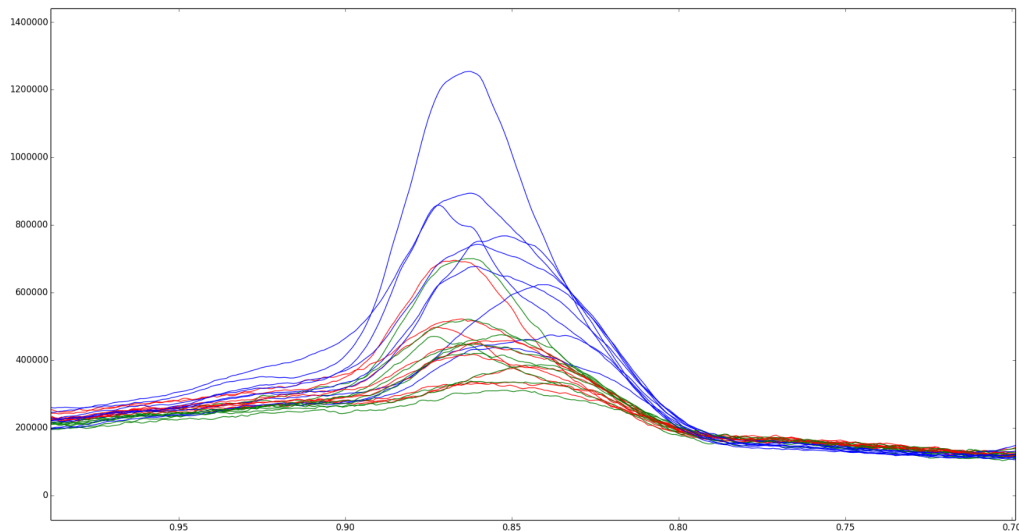


Figure 11. Spectrum obtained using the Bruker 600 MHz SampleJet, showing the different samples analyzed. The samples belonging to the Standard Protocol are shown in blue, the Optimized Protocol BSA 40 mg/mL in red, and the Optimized Protocol BSA 30 mg/mL in green. It can be observed that the baseline of the three groups is aligned.

In order to compare the results obtained from the different protocols studied, a series of statistical analyses were carried out, as explained in the previous section, and allowing us to observe the outcomes of this comparison. The following tables and figures summarize the main findings obtained during this phase of the study, enabling a clear visualization of the results and facilitating a direct comparison between the groups. The data obtained from the spectra processing and used to obtain the following results are included in the tables attached in Annex 1.

a. Concentration of Cholesterol:

Figures 12, 13, 14 and 15 provide the results corresponding to the cholesterol concentration (expressed in mg/dL) present in the main lipoprotein fractions (VLDL-C, IDL-C, LDL-C, and HDL-C).

The boxplots (the data used to obtain them are attached in Annex 3) in Figure 12 allow for the comparison of the distribution of the values obtained (previously normalized using Z-score) using three different protocols: the standard protocol (gray), the optimized protocol with BSA 40 mg/mL (yellow), and the optimized protocol with BSA 30 mg/mL (blue). The bolded points represent the outliers, and the numerical values displayed above the horizontal lines correspond to the p-values. In the case of VLDL-C, the medians are quite similar, although the protocol with BSA 40 shows greater data dispersion. For

IDL-C and LDL-C, the three groups exhibit similar values with comparable distributions. Finally, for HDL-C, it can be observed that the values from the protocol optimized with BSA 30 mg/mL show a lower median, with a higher presence of outliers and a different distribution compared to the other groups.

These results suggest that, overall, the protocols provide reliable results. Although HDL-C values show slight differences.

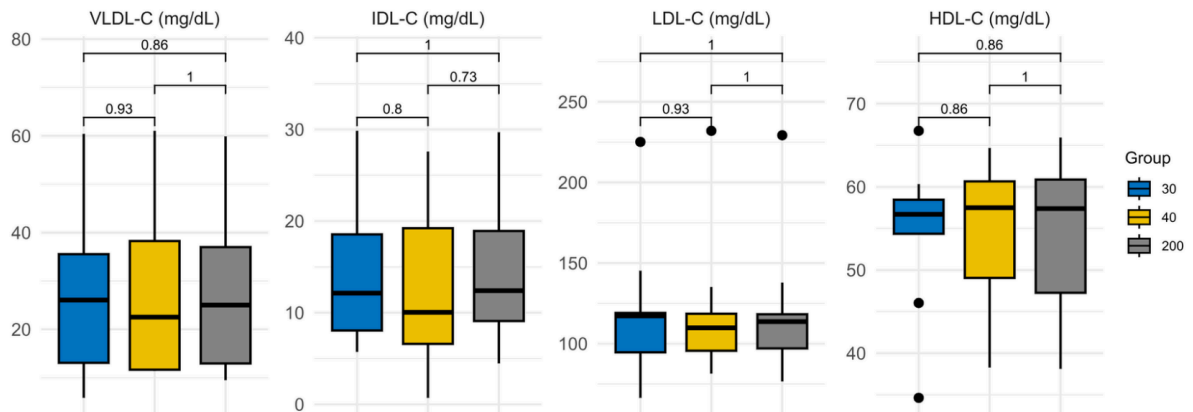


Figure 12. Boxplot representation of the data obtained through univariate analysis, showing the distribution of the values of the concentration of cholesterol present in each lipoprotein. In the figures, vertical black bars represent the standard deviations, and black dots indicate outliers, while the values above the brackets correspond to the p-values.

Figure 13 allows us to study the differences between the optimized protocols and the standard protocol, showing the difference between them relative to the average of the measurements. Each point represents one of the analyzed samples, with blue points corresponding to the difference between the optimized BSA 40 mg/mL protocol and the standard, and red points corresponding to the difference between the optimized BSA 30 mg/mL protocol and the standard. The red dashed lines indicate the standard deviation values for the optimized BSA 30 mg/mL protocol compared to the standard protocol, while the blue dashed line represents the same standard deviation in the case of the optimized BSA 40 mg/mL protocol. Finally, it should be noted that the red dashed line also represents the difference between the two compared values.

In most cases, the points can be seen to cluster around zero, suggesting that there is no significant difference between the samples analyzed using different protocols in comparison to the standard protocol. However, it can be observed that HDL-C values analyzed using the optimized BSA 30 mg/mL protocol show greater dispersion compared

to the other lipoproteins, which was also observed in the previous figure. Between the BSA protocols, some samples can be found pairing, mostly for the VLDL-C, reinforcing the comparability among them.

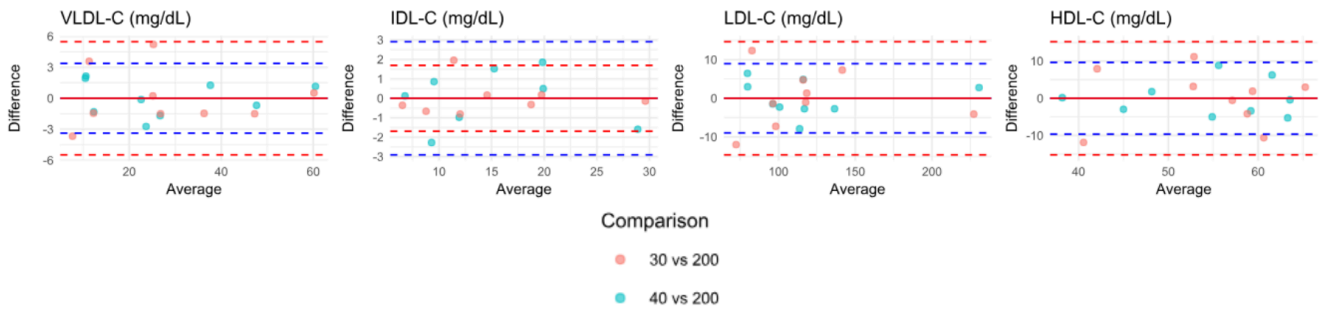


Figure 13. Graphical representation of the differences between protocols versus their mean of the concentration of cholesterol using the Bland-Altman method. Each point represents an individual sample, while the solid lines indicate the mean difference between protocols, and the dashed lines represent the corresponding standard deviations.

The correlation studies, as shown in Figures 14 and 15, suggest a very strong positive correlation in most fractions, except once again for HDL-C, which show a lower correlation coefficient (r) and a higher variance, compared to the others, in both the BSA 30 mg/mL and 40 mg/mL protocols.

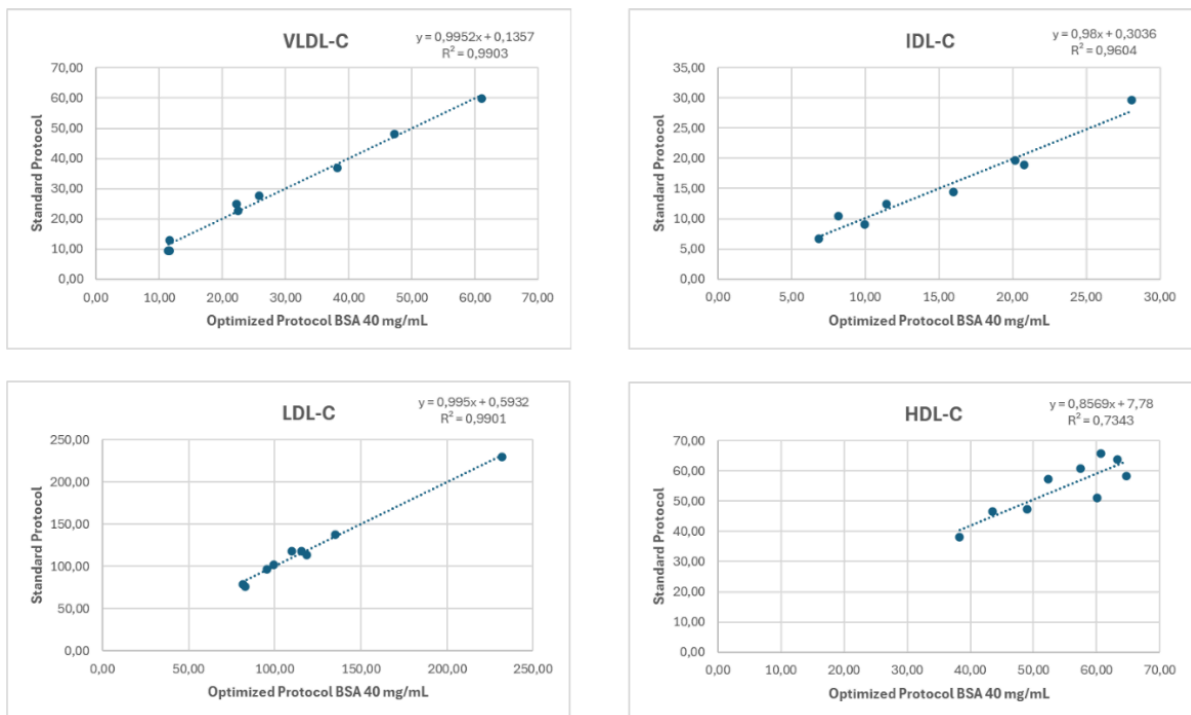


Figure 14. Regression lines showing the correlations between the concentrations of cholesterol under the standard protocol and the optimized protocols using BSA at 40 mg/mL, including their corresponding linear equations and correlation coefficients (r values).

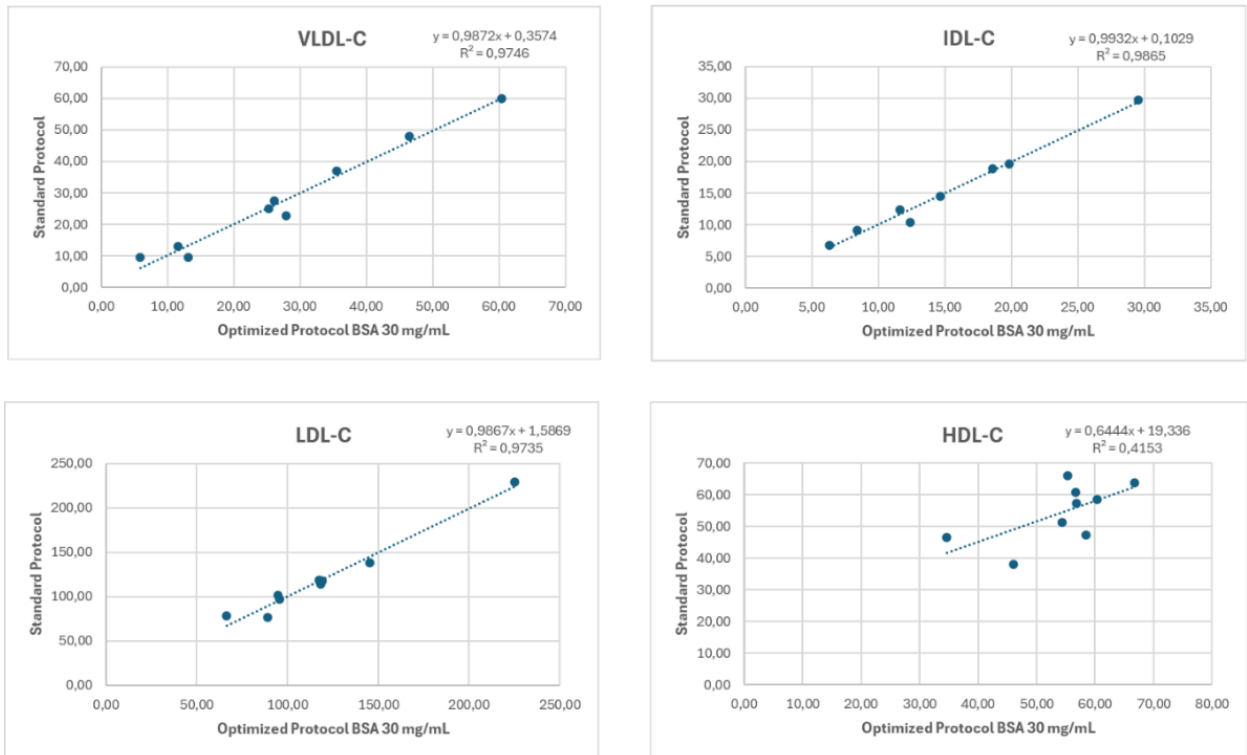


Figure 15. Regression lines showing the correlations between the concentrations of cholesterol under the standard protocol and the optimized protocols using BSA at 30 mg/mL, including their corresponding linear equations and correlation coefficients (r values).

b. Concentration of Triglycerides:

Figures 16, 17, 18 and 19 show the results corresponding to the triglyceride concentration (expressed in mg/dL) present in the main lipoprotein fractions (VLDL-TG, IDL-TG, LDL-TG, and HDL-TG).

In this case, as shown in Figure 16, most lipoprotein fractions present a similar and compact distribution of values with quite similar medians, except for IDL-TG, which shows some differences, although these are not statistically significant.

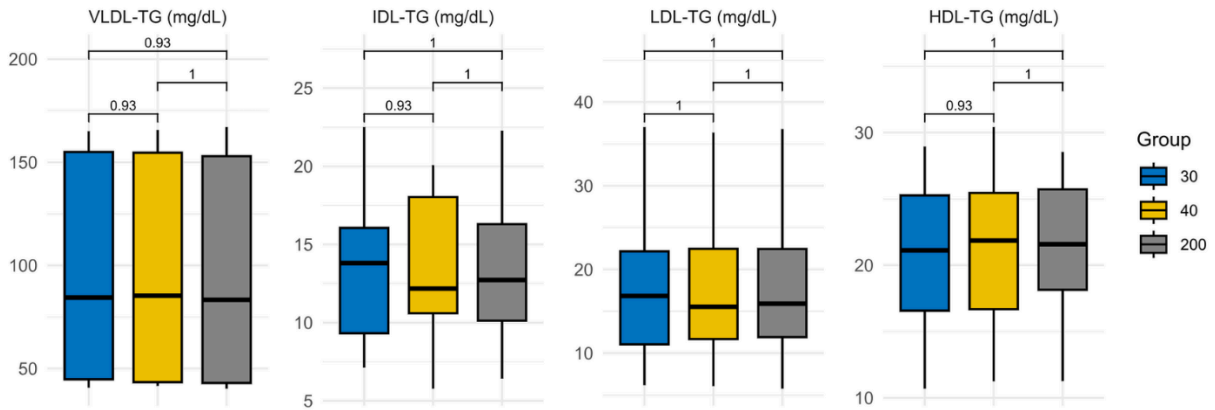


Figure 16. Boxplot representation of the data obtained through univariate analysis, showing the distribution of the values of the concentration of triglycerides present in each lipoprotein. In the figures, vertical black bars represent the standard deviations, and black dots indicate outliers, while the values above the brackets correspond to the p-values.

The Bland-Altman plots in Figure 17 show how the different points are distributed close to the zero line, indicating that the results provided by both protocols appear to be reliable.

The correlation studies shown in Figures 18 and 19 reflect a strong correlation between the optimized protocols and the standard, suggesting that the optimized protocol reproduces the results very consistently.

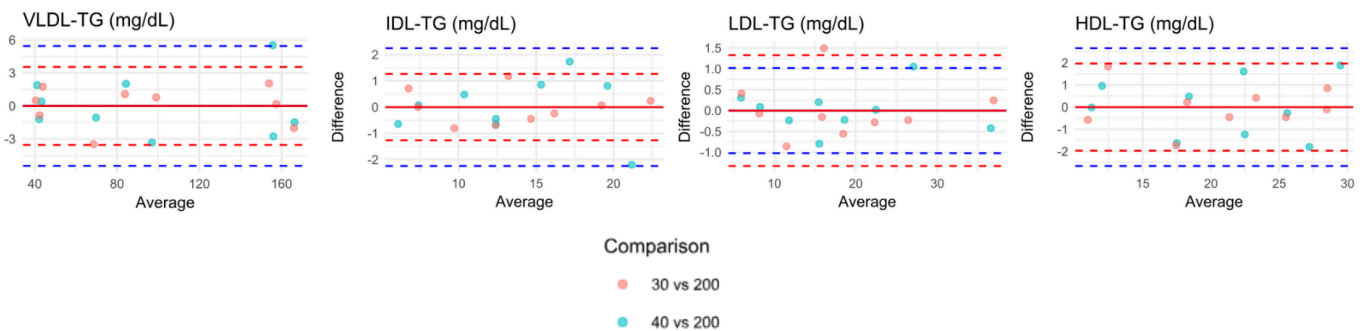


Figure 17. Graphical representation of the differences between protocols versus their mean of the concentration of triglycerides using the Bland-Altman method. Each point represents an individual sample, while the solid lines indicate the mean difference between protocols, and the dashed lines represent the corresponding standard deviations.

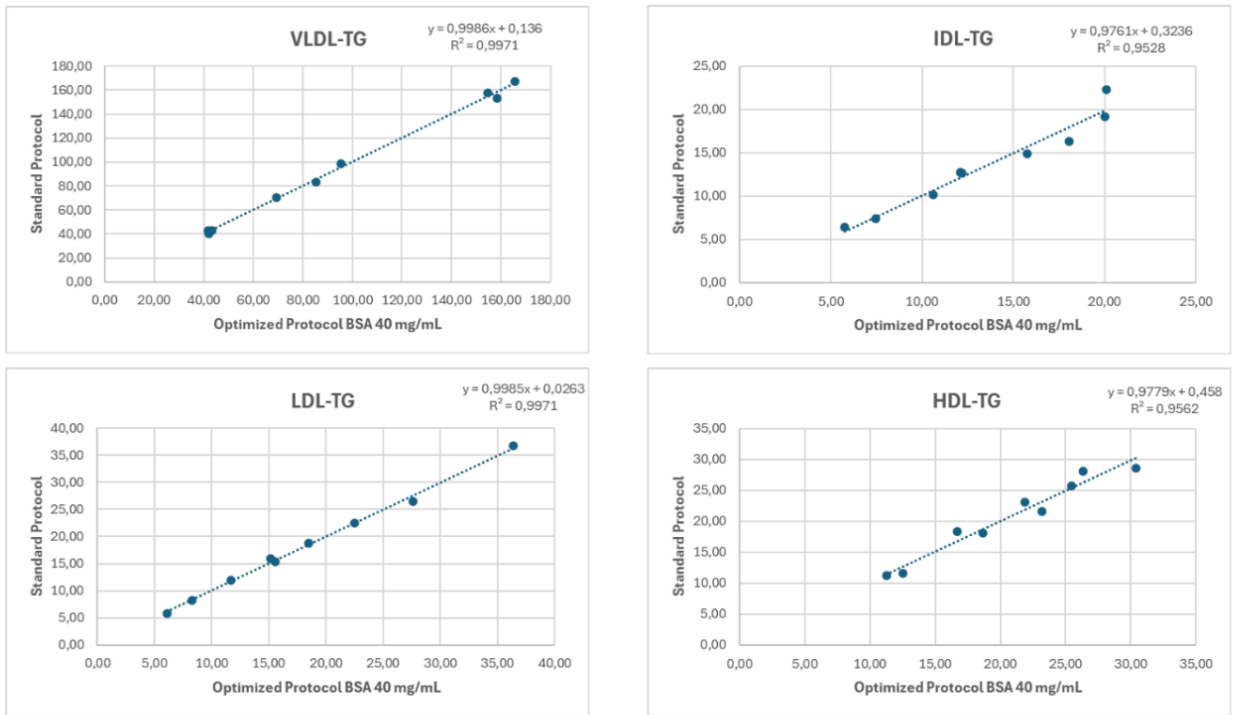


Figure 18. Regression lines showing the correlations between the concentrations of cholesterol under the standard protocol and the optimized protocols using BSA at 40 mg/mL, including their corresponding linear equations and correlation coefficients (r values).

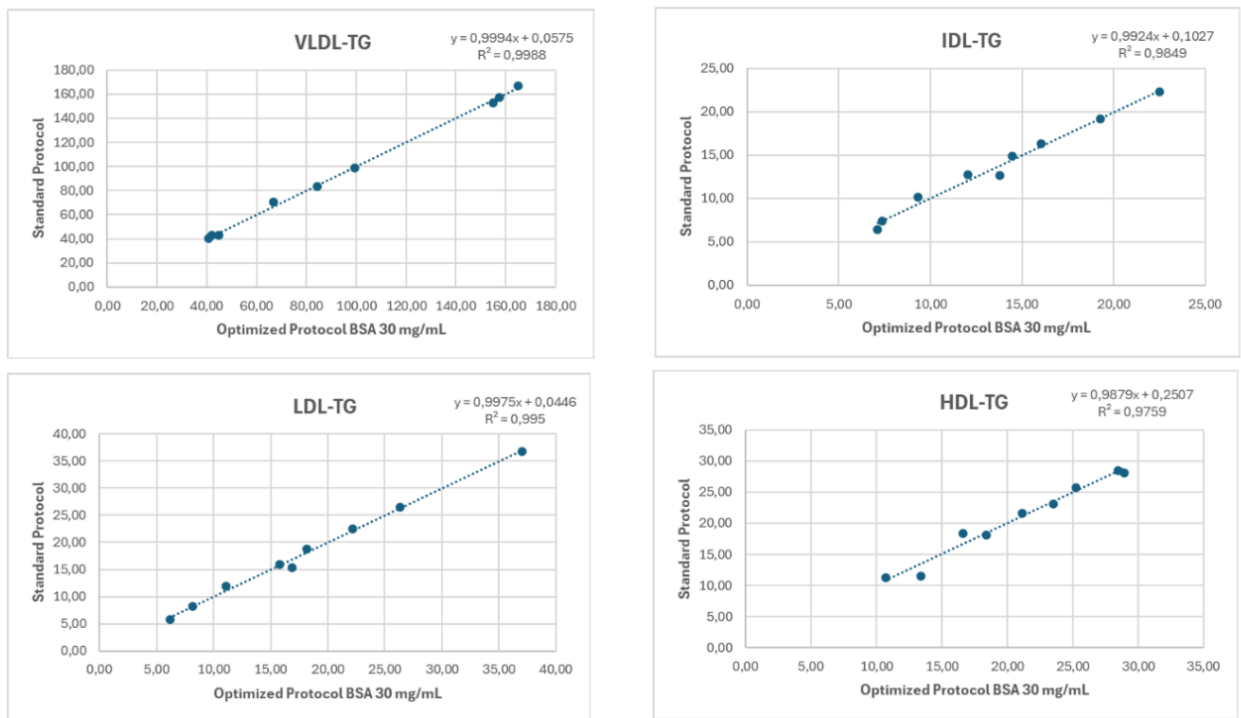


Figure 19. Regression lines showing the correlations between the concentrations of triglycerides under the standard protocol and the optimized protocols using BSA at 30 mg/mL, including their corresponding linear equations and correlation coefficients (r values).

c. Number of particles of lipoproteins and its subcategories:

Figures 20, 21, 22 and 23 show the quantification of the number of **VLDL** particles and their different subcategories: total, large, medium, and small (in nmol/L), using three different protocols. As can be seen in Figure 20, the median values are similar, and all groups display a fairly uniform distribution of values. The differences observed between the three groups do not appear to be statistically significant. This suggests that the optimized protocol does not alter the quantification of this parameter.

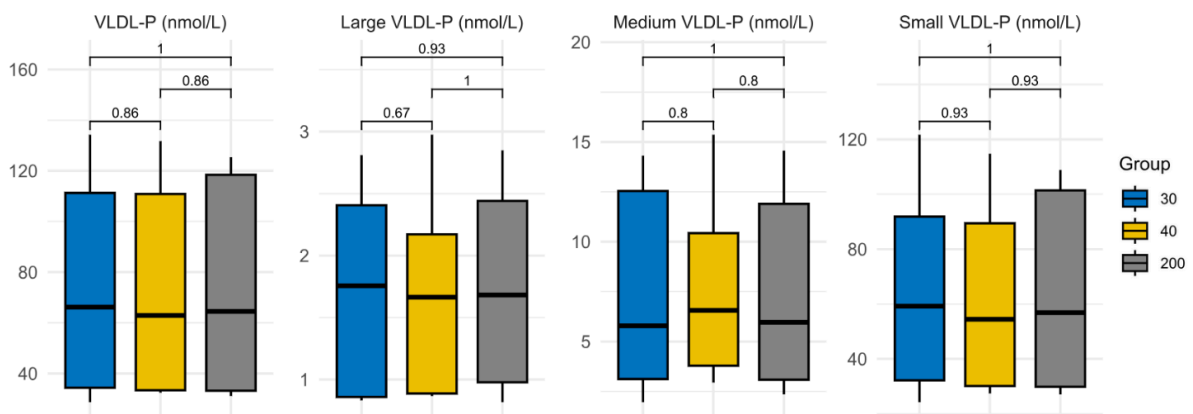


Figure 20. Boxplot representation of the data obtained through univariate analysis, showing the distribution of the values of the number of particles of VLDL present in each lipoprotein. In the figures, vertical black bars represent the standard deviations, and black dots indicate outliers, while the values above the brackets correspond to the p-values.

The Bland-Altman plots shown in Figure 21 corroborate what was suggested in the previous section. The points corresponding to the samples are dispersed around zero, with S-VLDL-P showing the greatest dispersion, although this is not statistically significant.

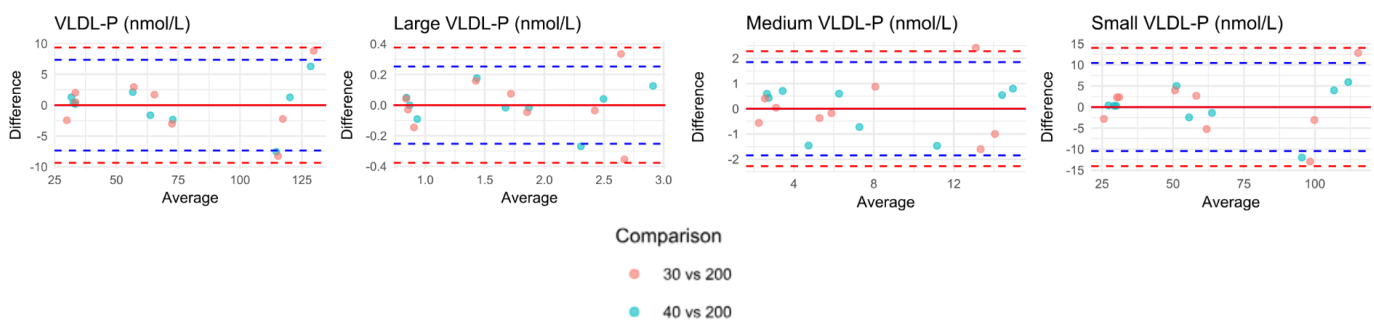


Figure 21. Graphical representation of the differences between protocols versus their mean of the number of particles of VLDL using the Bland-Altman method. Each point represents an individual sample, while the solid lines indicate the mean difference between protocols, and the dashed lines represent the corresponding standard deviations.

The correlation studies, shown in Figures 22 and 23, reveal highly significant correlations with an r value above 0.95 in most cases. It can also be observed that the correlation is

stronger in the optimized BSA 40 mg/mL protocol than in the BSA 30 mg/mL protocol as seen in the M-VLDL-P, for instance.

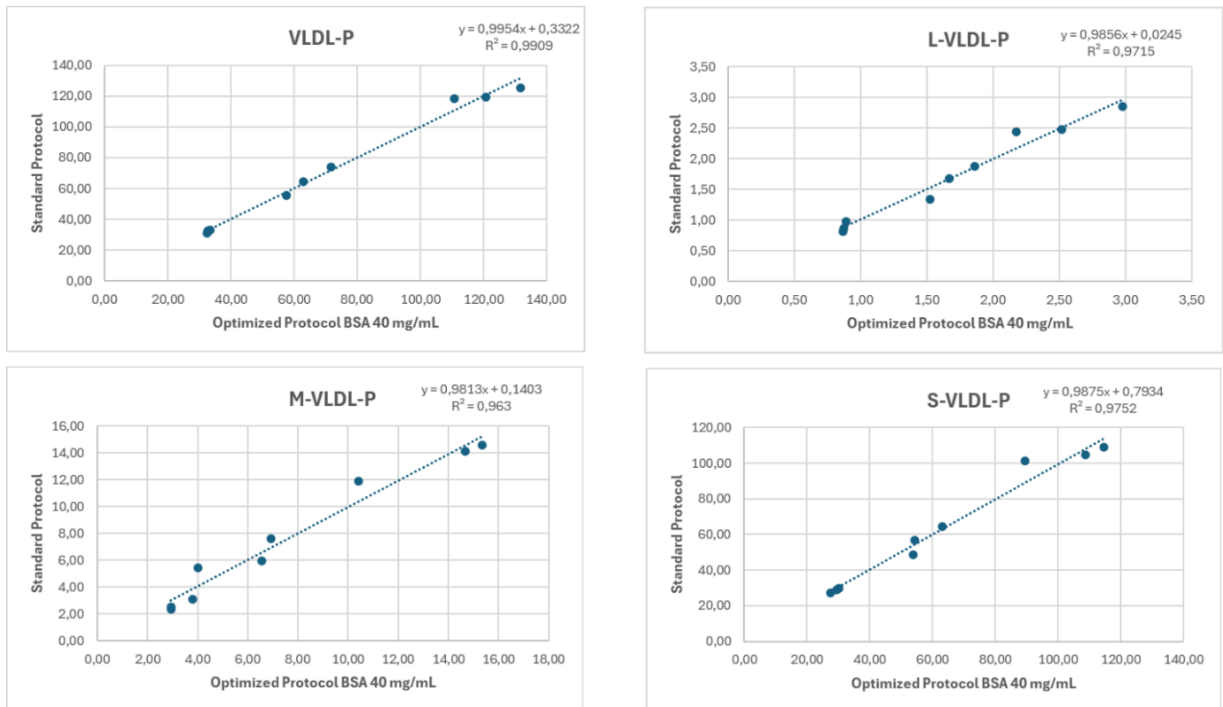


Figure 22. Regression lines showing the correlations between the number of particles of VLDL under the standard protocol and the optimized protocols using BSA at 40 mg/mL, including their corresponding linear equations and correlation coefficients (*r* values).

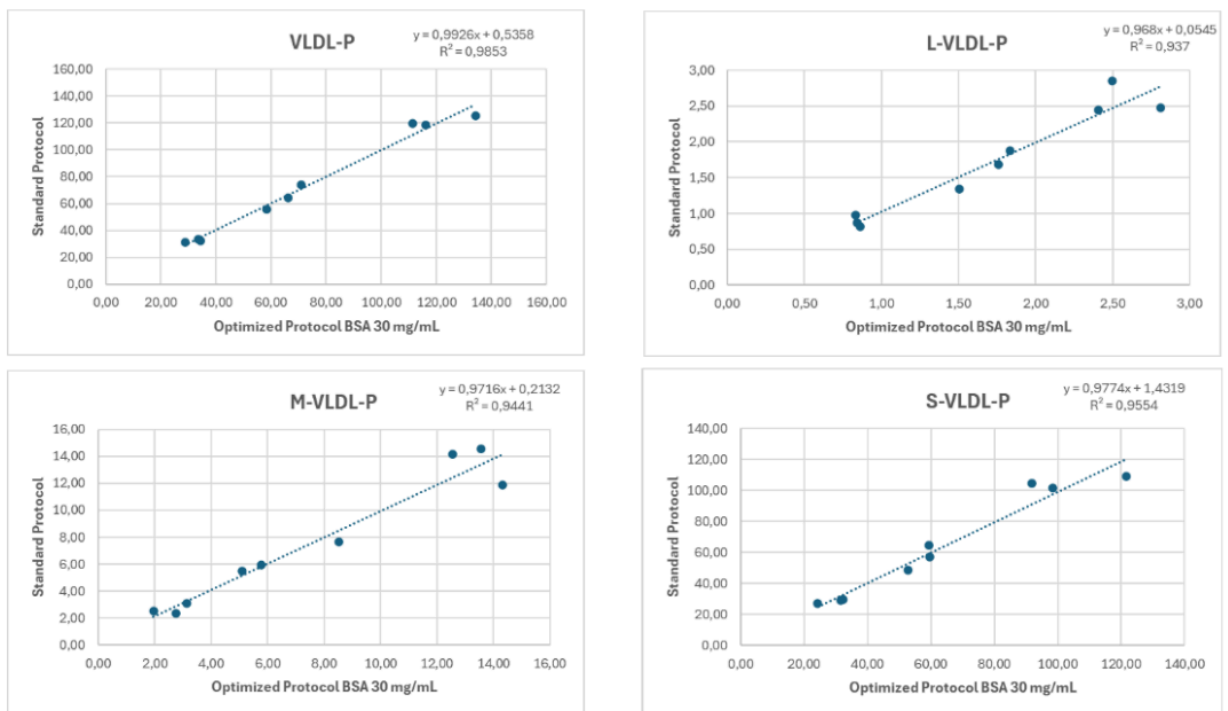


Figure 23. Regression lines showing the correlations between the number of particles of VLDL under the standard protocol and the optimized protocols using BSA at 30 mg/mL, including their corresponding linear equations and correlation coefficients (*r* values).

Figures 24, 25, 26 and 27 represent the quantification of the number of **LDL** particles and their different subcategories: total, large, medium, and small (in nmol/L), using three different protocols. As can be seen in Figure 24, the median values are similar, and all groups show a fairly uniform distribution of values except for M-LDL-P. The differences observed between the three groups do not appear to be statistically significant. This suggests that the optimized protocol does not alter the quantification of this parameter.

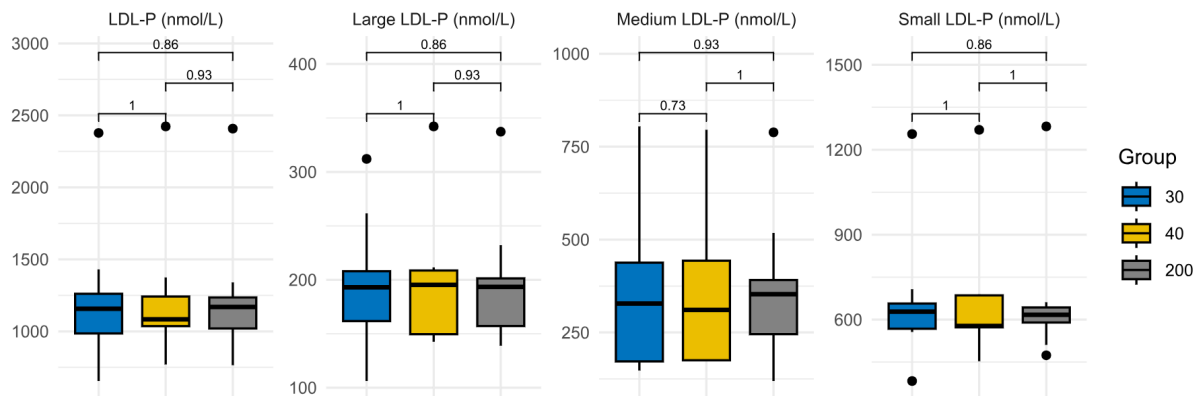


Figure 24. Boxplot representation of the data obtained through univariate analysis, showing the distribution of the values of the number of particles of LDL present in each lipoprotein. In the figures, vertical black bars represent the standard deviations, and black dots indicate outliers, while the values above the brackets correspond to the p-values.

The Bland-Altman plots shown in Figure 25 corroborate what was suggested in the previous section. The points corresponding to the samples are dispersed around zero, with M-LDL-P showing the greatest dispersion, although this is not statistically significant.

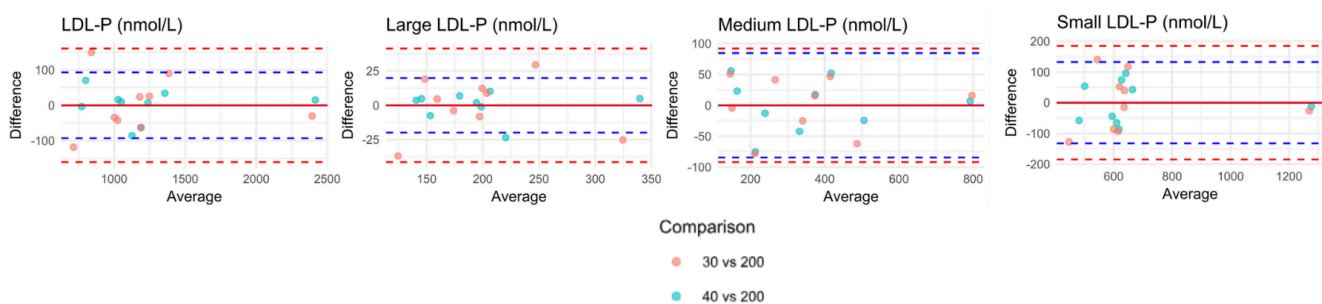


Figure 25. Graphical representation of the differences between protocols versus their mean of the number of particles of LDL using the Bland-Altman method. Each point represents an individual sample, while the solid lines indicate the mean difference between protocols, and the dashed lines represent the corresponding standard deviations.

The correlation studies, shown in Figures 26 and 27, reveal highly significant correlations with an r-value greater than 0.95 in most cases. It can also be observed that the correlation is stronger in the optimized BSA 40 mg/mL protocol than in the BSA 30

mg/mL protocol. In addition, it can be appreciated that the protocols proposed respect the quantification across a broad concentration range.

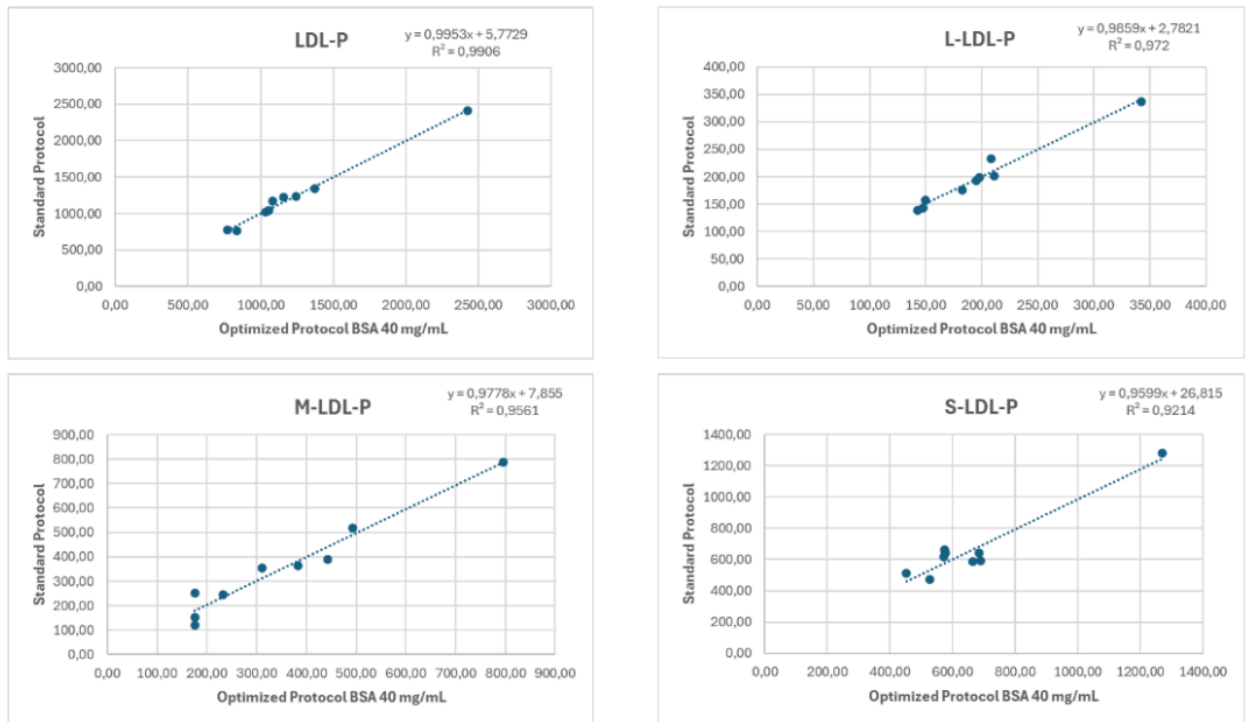


Figure 26. Regression lines showing the correlations between the number of particles of LDL under the standard protocol and the optimized protocols using BSA at 40 mg/mL, including their corresponding linear equations and correlation coefficients (r values).

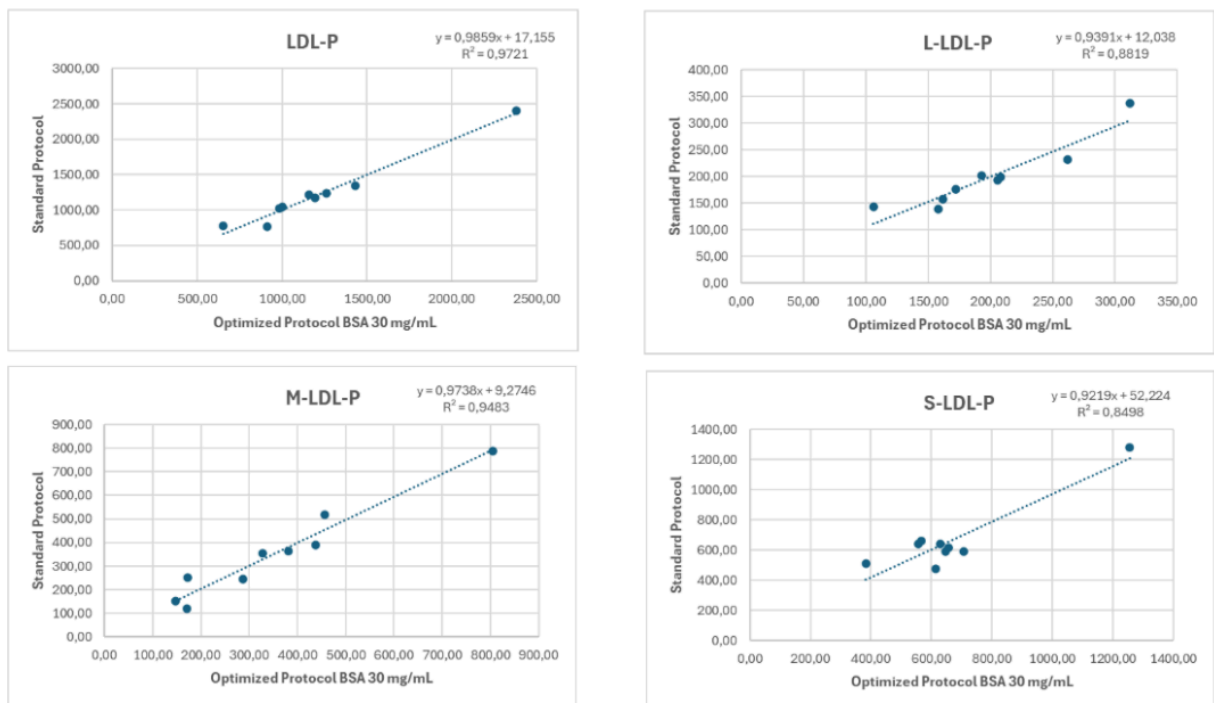


Figure 27. Regression lines showing the correlations between the number of particles of LDL under the standard protocol and the optimized protocols using BSA at 30 mg/mL, including their corresponding linear equations and correlation coefficients (r values).

Figures 28 and 29 represent the quantification of the number of HDL particles and their different subcategories: total, large, medium, and small (in nmol/L), using three different protocols. It is worth noting that, as shown in the attached Tables 7 and 8 (annex) , the values obtained for L-HDL-P and S-HDL-P through the proposed protocols are negligible, as they are close to zero. Therefore, although after Z-score normalization the data may appear to have a similar distribution, these values should not be taken into account.

For this same reason, the discussion will focus only on the correlation studies shown in Figures 28 and 29, which reveal significant correlations with an r value above 0.8 for M-HDL-P, while for the other two subcategories the value reaches 0. It can also be observed that, unlike the other parameters, the correlation is stronger in the optimized BSA 30 mg/mL protocol than in the BSA 40 mg/mL protocol.

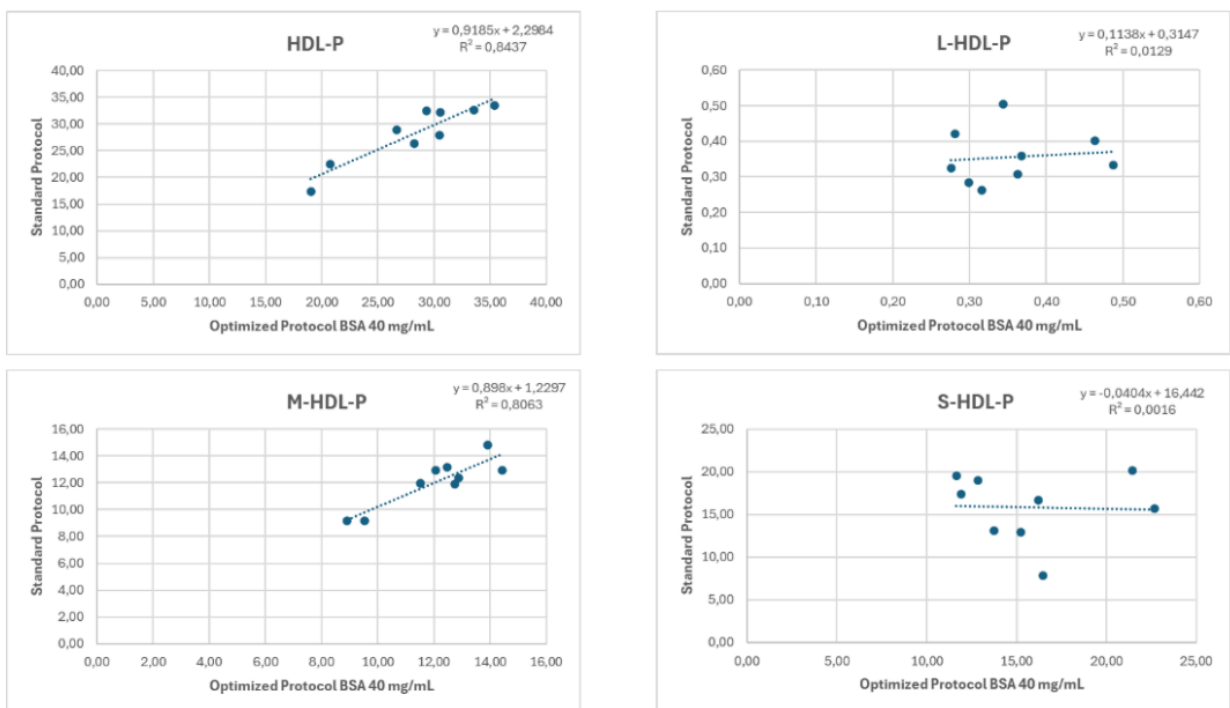


Figure 28. Regression lines showing the correlations between the number of particles of HDL under the standard protocol and the optimized protocols using BSA at 40 mg/mL, including their corresponding linear equations and correlation coefficients (r values).

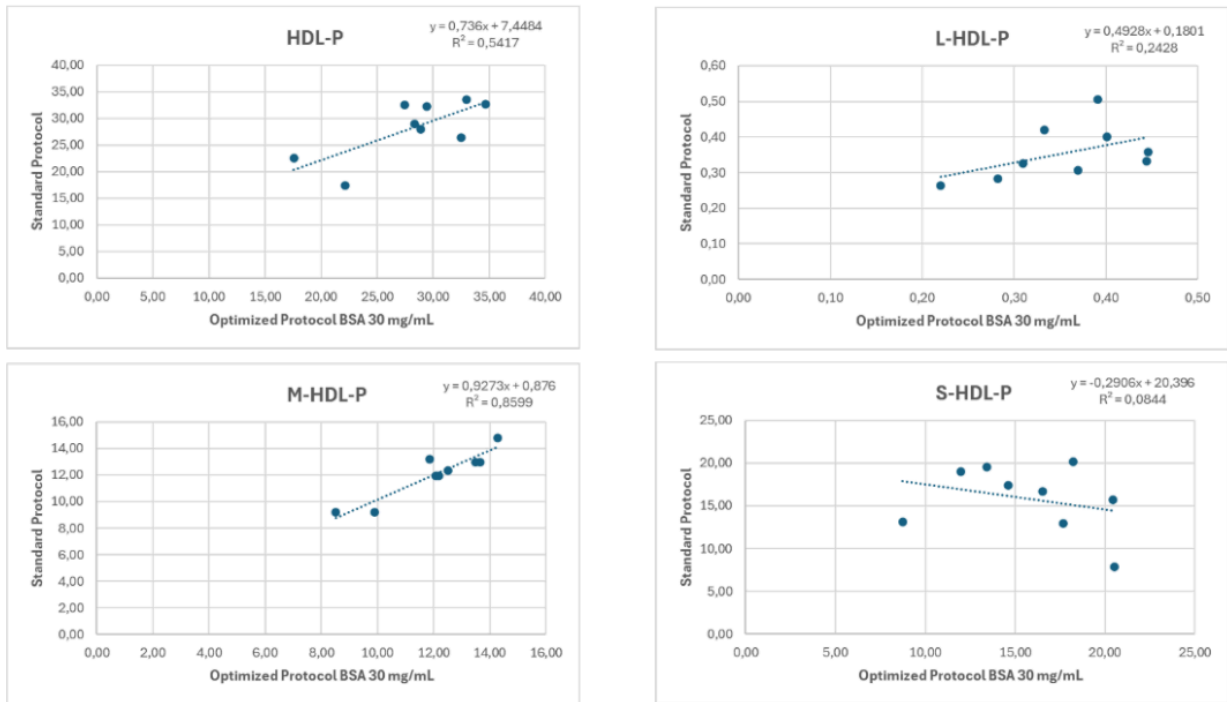


Figure 29. Regression lines showing the correlations between the number of particles of HDL under the standard protocol and the optimized protocols using BSA at 30 mg/mL, including their corresponding linear equations and correlation coefficients (r values).

d. Average size of particles:

Figures 30, 31, 32 and 33 represent the determination of the average size of the different lipoprotein subfractions (VLDL, LDL, and HDL) in nanometers using three different protocols.

As can be seen in Figure 30, the median values are similar, and all groups show a fairly uniform distribution of values. The differences observed between the three groups do not appear to be statistically significant. It should also be noted that if there appears to be greater dispersion, it is because the magnitude of these variables is smaller, or in other words, the range of the variables is narrower. This suggests that the optimized protocol does not alter the quantification of this parameter.

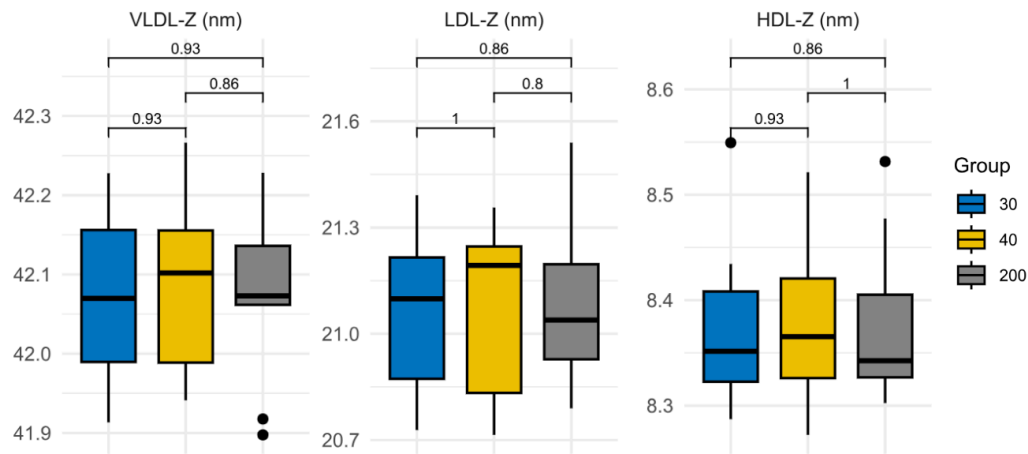


Figure 30. Boxplot representation of the data obtained through univariate analysis, showing the distribution of the values of the average size of each lipoprotein. In the figures, vertical black bars represent the standard deviations, and black dots indicate outliers, while the values above the brackets correspond to the p-values.

The Bland-Altman plots shown in Figure 31 corroborate what was suggested in the previous section. The points corresponding to the samples are dispersed around zero, with the standard deviations of both samples being so similar that, in some cases, they even overlap.

The correlation studies shown in Figures 32 and 33 reveal weak correlations, with r values ranging between 0.2 and 0.5 depending on the sample. It is difficult to achieve high values of r since this parameter operates on a smaller scale. It appears that the parameter with the best correlation is LDL-Z. It can also be observed that the correlation is stronger in the optimized BSA 40 mg/mL protocol than in the BSA 30 mg/mL protocol.

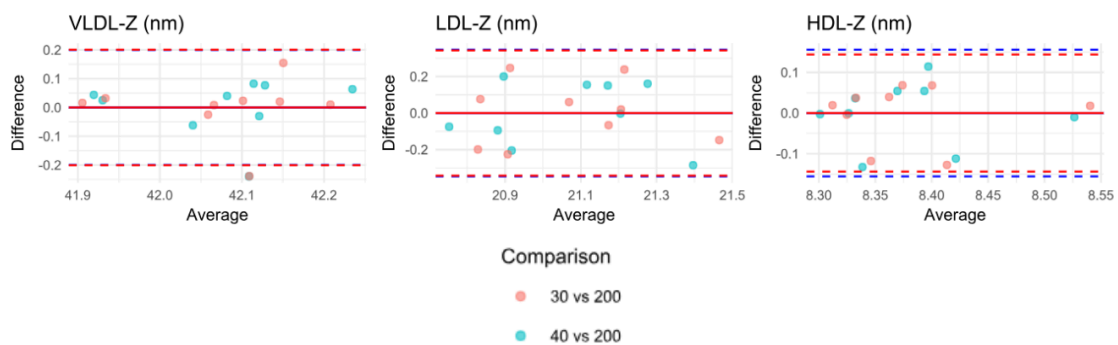


Figure 31. Graphical representation of the differences between protocols versus their mean of the average size of each lipoprotein using the Bland-Altman method. Each point represents an individual sample, while the solid lines indicate the mean difference between protocols, and the dashed lines represent the corresponding standard deviations.

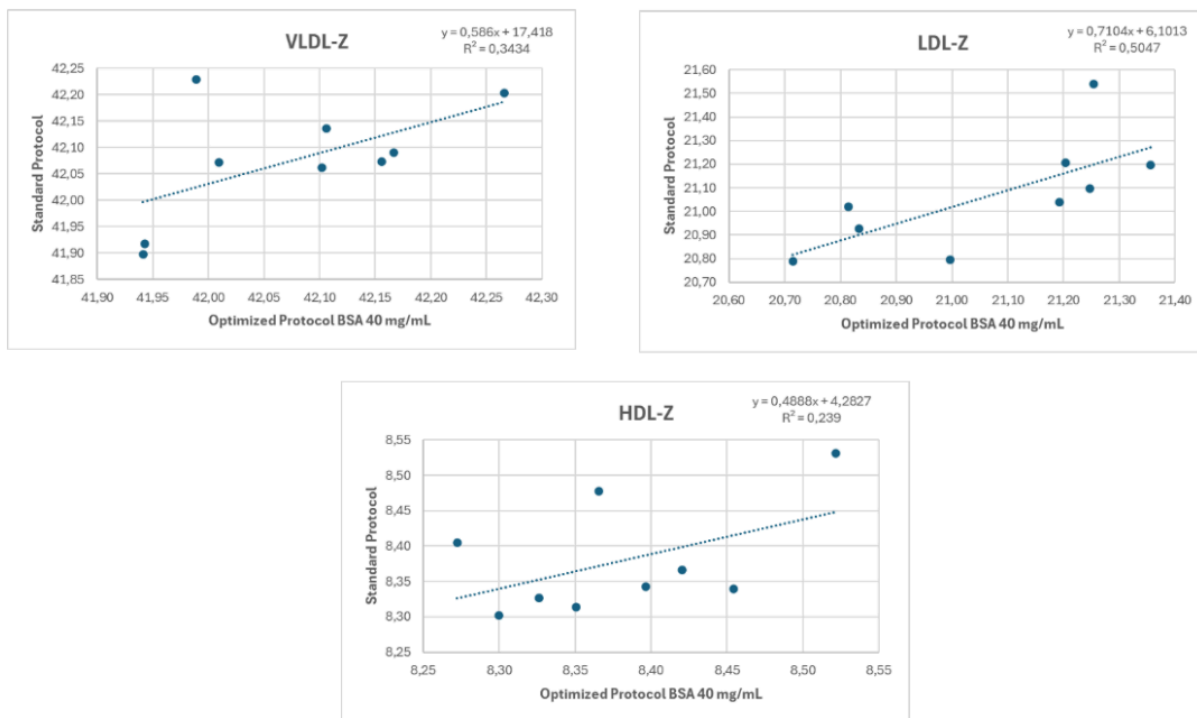


Figure 32. Regression lines showing the correlations between the average size of each lipoprotein under the standard protocol and the optimized protocols using BSA at 40 mg/mL, including their corresponding linear equations and correlation coefficients (r values).

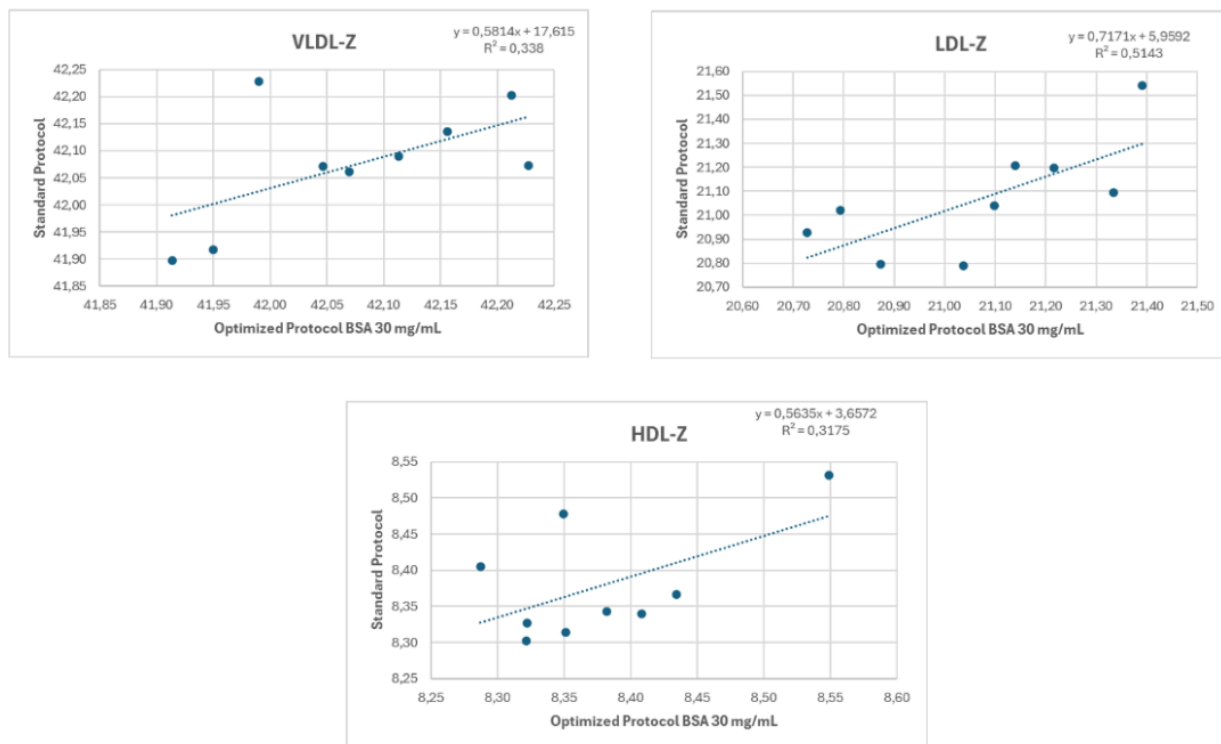


Figure 33. Regression lines showing the correlations between the average size of each lipoprotein under the standard protocol and the optimized protocols using BSA at 30 mg/mL, including their corresponding linear equations and correlation coefficients (r values).

- e. **Relative distribution of lipoproteins:** The reliability of this parameter depends on the results obtained previously, as can be seen in the formula mentioned in section 2.2. Therefore, it is not relevant to carry out a comparative study of the protocols used.

6. DISCUSSION:

It is important to emphasize the relevance of optimizing this protocol to enable work with reduced sample volumes, given the limitations these pose when conducting clinical analyses or research studies. The use of the optimized protocol allows for reduced operational costs, minimized required sample volume, and expanded applicability of the technique in vulnerable populations or contexts where the available volume is limited. Therefore, this study aims to optimize the standard protocol used for the quantification of lipoproteins by ¹H-NMR spectroscopy without compromising the analytical precision of the method.

The results obtained in this study suggest that it is possible to use the optimized protocol for reduced-volume samples, although there are some limitations.

Comparisons made between the standard protocol and the optimized protocols (BSA 30 mg/mL and 40 mg/mL) revealed a high correlation across all evaluated parameters, including lipid concentration, particle number, average size, and subclass distribution.

A study published in the *Journal of Proteome Research* assessed the feasibility of performing quantitative lipoprotein analyses using 3 mm NMR tubes (0.1 mL of plasma) compared to the standard 5 mm tubes (0.3 mL of plasma). The results showed a high correlation ($R^2 > 0.95$) between both formats for most lipoprotein parameters, including total cholesterol, LDL-C, and HDL-C [10].

Most of the compared parameters showed consistent and reliable results. In the case of cholesterol and triglyceride concentrations, the findings suggest no significant differences between the values obtained using both protocols, indicating that the optimized protocol is reliable. Linear regressions showed correlation coefficients (r) greater than 0.9 in most cases, and Bland-Altman analyses confirmed the absence of relevant systematic bias.

It is important to note that HDL-C results were not consistent. This is due to the fact that the Liposcale software has defined ranges for each variable that are triggered when the results obtained surpass a certain threshold. Since the spectra acquired using the optimized protocols show significantly lower intensities than usual, their computed results are consequently lower than usual and therefore assigned the minimum value detectable by the technique. Therefore, in the case of HDL-C, as values fall below the defined range for the technique, there is poor correlation between the two protocols. To address this issue, the software would need to be optimized to accommodate lower value ranges.

The same applies to parameters such as the number of lipoprotein particles and their subcategories. In most cases, results suggest no significant difference between values obtained by both protocols, indicating that the optimized protocol is reliable. Linear regressions showed high correlation coefficients (r) in most cases, and Bland-Altman analyses confirmed the absence of relevant systematic bias.

An exception to this are the M-HDL-P and S-HDL-P, for which software optimization or reconfiguration is required. As previously mentioned, the spectra obtained via the optimized protocol show lower-than-usual intensity. Particle number is determined by deconvolution processes, which are carried out through mathematical estimations/approximations that decompose the original signal into contributions from each lipoprotein and its subcategories. Due to the lower intensity, some signals do not match properly, preventing reliable results from being obtained. In order to generate accurate results for these parameters, the software would need to be optimized or reconfigured.

It is also worth highlighting that the stability of the average particle size between protocols reinforces the robustness of the optimized approach. Given that this parameter is clinically relevant, especially in the case of LDL, its invariance suggests that the quality of the lipid profile is not affected by the reduced sample volume.

This study also investigated how varying albumin concentration affects result resolution, and as shown in the figures included in the previous section, there is no significant difference between the two optimized protocols. This allows us to conclude that both options are viable and produce consistent results.

These findings are consistent with previous studies that demonstrated the feasibility of using NMR protocols with an albumin concentration of 40 mg/mL, which helps maintain sample viscosity, an important property during NMR measurements, even when working with small volumes. This study contributes added value to the literature by working with reduced sample volumes and testing various albumin concentrations to assess their effect on resolution [9].

Implementing this optimized protocol represents a significant advantage, especially in clinical and experimental settings where sample volume is limited, as it allows lipoprotein quantification via NMR while maintaining analytical robustness and reducing operational and reagent costs.

However, it is also important to acknowledge the limitations of this study. First, the sample size ($n=9$) is a significant constraint. Although efforts were made to cover a range of lipid concentrations, it would be necessary to validate these findings in a larger and more

heterogeneous cohort. Secondly, software optimization is needed to obtain reliable results for all parameters.

In summary, the data obtained demonstrate that the optimized protocols using albumin at 30 and 40 mg/mL suggest that it is possible to perform comprehensive and reliable lipoprotein characterization by ¹H-NMR using a significantly smaller sample volume than is typically required. This optimization does not appear to compromise result quality and opens up new possibilities for implementation in contexts where sample volume is a significant limitation.

7. CONCLUSIONS:

This study suggests that it is possible to optimize a lipoprotein quantification protocol using ¹H-NMR spectroscopy with reduced sample volumes without compromising the analytical accuracy of the method.

Comparisons made between the standard protocol and the optimized protocols (BSA 30 mg/mL and 40 mg/mL) suggest a high correlation across all evaluated parameters, including lipid concentration, particle number, average sizes, and subclass distribution.

No significant differences were found between the optimized protocols using albumin at 30 mg/mL and 40 mg/mL, indicating that there is no meaningful relationship between BSA concentration and result resolution. Both concentrations are valid and appear to yield consistent results.

Moreover, the use of reduced sample volumes for the Liposcale® test represents a novel advancement, as this methodology had not previously been applied under limited sample conditions.

Despite the promising results, the limited sample size (n=9) represents a significant limitation. Therefore, it is recommended to validate these findings in a larger and more heterogeneous cohort, as well as to improve the sensitivity of the software for analyzing low-intensity signals.

8. BIBLIOGRAPHY:

- [1] K. R. Feingold, *Introduction to Lipids and Lipoproteins*, N/A. South Dartmouth: MDText.com, Inc., 2000.
- [2] B. A. Ference *et al.*, “Low-density lipoproteins cause atherosclerotic cardiovascular disease. 1. Evidence from genetic, epidemiologic, and clinical studies. A consensus statement from the European Atherosclerosis Society Consensus Panel,” *Eur Heart J*, vol. 38, no. 32, pp. 2459–2472, Aug. 2017, doi: 10.1093/eurheartj/ehx144.
- [3] World Health Organization, “Cardiovascular diseases (CVDs),” World Health Organization. Accessed: Apr. 04, 2025. [Online]. Available: [https://www.who.int/news-room/fact-sheets/detail/cardiovascular-diseases-\(cvds\)](https://www.who.int/news-room/fact-sheets/detail/cardiovascular-diseases-(cvds))
- [4] R. Mallol *et al.*, “Liposcale: a novel advanced lipoprotein test based on 2D diffusion-ordered 1H NMR spectroscopy,” *J Lipid Res*, vol. 56, no. 3, pp. 737–746, Mar. 2015, doi: 10.1194/jlr.D050120.
- [5] E. U. Emeasoba, E. Ibeson, I. Nwosu, N. Montemarano, J. Shani, and V. S. Shetty, “Clinical Relevance of Nuclear Magnetic Resonance LipoProfile,” *Frontiers in Nuclear Medicine*, vol. 2, Jul. 2022, doi: 10.3389/fnume.2022.960522.
- [6] A. Barron, “NMR Spectroscopy,” LibreTexts. Accessed: Apr. 04, 2025. [Online]. Available: [https://chem.libretexts.org/Bookshelves/Analytical_Chemistry/Physical_Methods_in_Chemistry_and_Nano_Science_\(Barron\)/04%3A_Chemical_Speciation/4.07%3A_NMR_Spectroscopy](https://chem.libretexts.org/Bookshelves/Analytical_Chemistry/Physical_Methods_in_Chemistry_and_Nano_Science_(Barron)/04%3A_Chemical_Speciation/4.07%3A_NMR_Spectroscopy)
- [7] P. Soinenen *et al.*, “High-throughput serum NMR metabolomics for cost-effective holistic studies on systemic metabolism,” *Analyst*, vol. 134, no. 9, p. 1781, 2009, doi: 10.1039/b910205a.
- [8] X. Pintó *et al.*, “Documento de consenso de un grupo de expertos de la Sociedad Española de Arteriosclerosis (SEA) sobre el uso clínico de la resonancia magnética nuclear en el estudio del metabolismo lipoproteico (Liposcale),” *Clínica e Investigación en Arteriosclerosis*, vol. 32, no. 5, pp. 219–229, Sep. 2020, doi: 10.1016/j.arteri.2020.04.004.
- [9] C. DUDUIANU, A. NICOLESCU, M. CRISTEA, R. STAN, and C. DELEANU, “NMR proven albumin interaction with metabolites in complex mixtures,” *Revue Roumaine de Chimie*, vol. 68, no. 5–6, pp. 253–259, May 2023, doi: 10.33224/rch.2023.68.5-6.08.
- [10] S. Lodge *et al.*, “Low Volume in Vitro Diagnostic Proton NMR Spectroscopy of Human Blood Plasma for Lipoprotein and Metabolite Analysis: Application to SARS-CoV-2 Biomarkers,” *J Proteome Res*, vol. 20, no. 2, pp. 1415–1423, Feb. 2021, doi: 10.1021/acs.jproteome.0c00815.

9. ANNEXES:

9.1. ANNEX 1:

Table 3. Quantification of cholesterol and triglyceride concentrations in lipoproteins using the standard protocol.

Standard Protocol (200 µL)	Cholesterol (mg/dL)				Triglycerides (mg/dL)			
	VLDL	IDL	LDL	HDL	VLDL	IDL	LDL	HDL
Sample Low 1	37,01	10,43	97,09	51,19	167,08	12,63	15,34	23,10
Sample Low 2	59,89	29,69	229,28	47,27	152,94	22,27	36,77	28,10
Sample Low 3	48,01	19,66	113,71	58,43	157,40	19,20	26,54	28,54
Sample Med 1	22,65	18,92	137,91	63,75	70,31	16,30	22,45	25,72
Sample Med 2	25,03	12,40	117,76	57,39	83,33	12,73	15,92	18,15
Sample Med 3	27,55	14,48	118,27	60,88	98,62	14,90	18,72	21,58
Sample High 1	9,52	4,47	78,43	46,48	43,01	6,42	5,76	11,27
Sample High 2	9,51	6,70	76,58	38,11	42,75	7,38	8,20	11,54
Sample High 3	12,96	9,10	101,89	65,93	40,24	10,13	11,92	18,31

Table 4. Quantification of cholesterol and triglyceride concentrations in lipoproteins using the Optimized Protocol (BSA 30 mg/mL).

Optimized Protocol (BSA 30 mg/mL)	Cholesterol (mg/dL)				Triglycerides (mg/dL)			
	VLDL	IDL	LDL	HDL	VLDL	IDL	LDL	HDL
Sample Low 1	20,60	4,90	67,35	41,43	84,78	5,68	6,46	15,78
Sample Low 2	32,35	13,03	135,02	43,79	80,64	9,76	15,48	18,67
Sample Low 3	25,78	8,43	79,24	44,88	81,70	8,24	10,70	18,39
Sample Med 1	16,97	7,85	93,22	48,58	44,43	6,74	8,84	16,71
Sample Med 2	15,74	4,53	79,55	42,86	51,65	4,86	5,98	13,06
Sample Med 3	16,12	5,98	78,59	42,78	57,80	5,98	7,05	14,52
Sample High 1	6,57	1,96	52,02	30,03	35,36	2,56	1,70	8,99
Sample High 2	9,99	2,04	63,79	36,62	34,19	2,68	2,57	10,41

Optimized Protocol (BSA 30 mg/mL)	Cholesterol (mg/dL)				Triglycerides (mg/dL)			
	VLDL	IDL	LDL	HDL	VLDL	IDL	LDL	HDL
Sample Low 1	20,60	4,90	67,35	41,43	84,78	5,68	6,46	15,78
Sample Low 2	32,35	13,03	135,02	43,79	80,64	9,76	15,48	18,67
Sample Low 3	25,78	8,43	79,24	44,88	81,70	8,24	10,70	18,39
Sample High 3	9,25	3,03	66,77	41,98	33,71	3,59	3,88	12,11

*Table 5. Quantification of cholesterol and triglyceride concentrations in lipoproteins using the Optimized Protocol (BSA 40 mg/mL). *Out of limit detection (Due to the IDL-C parameter of one of the samples was outside the detection limit, none of the results for that parameter from that sample were taken into account for the statistical analyses.)*

Optimized Protocol (BSA 40 mg/mL)	Cholesterol (mg/dL)				Triglycerides (mg/dL)			
	VLDL	IDL	LDL	HDL	VLDL	IDL	LDL	HDL
Sample Low 1	20,41	1,97	57,74	35,99	83,92	3,45	4,88	12,63
Sample Low 2	30,53	9,00	115,26	31,93	80,95	6,15	12,88	14,28
Sample Low 3	24,43	6,20	67,43	37,71	79,35	6,13	9,51	15,80
Sample Med 1	13,42	6,41	74,42	37,21	43,73	5,45	7,54	13,96
Sample Med 2	13,31	3,12	63,73	33,16	50,45	3,42	4,72	11,43
Sample Med 3	14,90	4,74	66,14	35,05	54,59	4,67	6,01	13,13
Sample High 1	8,59	-*	51,75	29,89	32,96	1,26	1,24	8,70
Sample High 2	8,49	1,50	52,44	27,95	32,18	1,84	2,09	9,16
Sample High 3	8,58	2,60	59,42	36,22	32,43	2,91	3,40	10,71

Table 6. Determination of the particle number corresponding to each lipoprotein and its associated subcategories using the Standard Protocol.

Standard Protocol	VLDL (nmol/L)				LDL (nmol/L)				HDL (μ mol/L)			
	P	L	M	S	P	L	M	S	P	L	M	S
Sample Low 1	119,5	2,85	11,90	104,8	1046	157,1	245,5	642,9	27,93	0,33	11,93	15,67
Sample Low 2	125,4	2,44	14,15	108,8	2408	337,3	788,7	1282	26,34	0,50	12,94	12,90

Sample Low 3	118,4	2,48	14,56	101,4	1235	201,3	391,2	642,9	33,52	0,40	12,96	20,16
Sample Med 1	55,56	1,34	5,46	48,75	1339	232,1	517,9	589,8	32,59	0,42	14,80	17,37
Sample Med 2	64,54	1,68	5,96	56,89	1169	199,1	353,1	617	28,92	0,31	11,94	16,68
Sample Med 3	73,98	1,88	7,64	64,46	1220	193	365	661	32,21	0,33	12,35	19,54
Sample High 1	31,14	0,98	3,09	27,08	773,4	143,1	119,5	510,8	22,55	0,26	9,19	13,10
Sample High 2	32,37	0,87	2,35	29,15	765,1	138,9	152,1	474,	17,38	0,36	9,18	7,83
Sample High 3	33,21	0,82	2,52	29,87	1020	175,9	250,5	593,6	32,45	0,28	13,18	18,99

Table 7. Determination of the particle number corresponding to each lipoprotein and its associated subcategories using the Optimized Protocol (BSA 30 mg/mL).

Optimized Protocol (BSA 30 mg/mL)	VLDL (nmol/L)				LDL (nmol/L)				HDL (μmol/L)			
	P	L	M	S	P	L	M	S	P	L	M	S
Sample Low 1	56,59	1,79	9,11	45,69	663,1	145,7	72,01	445,4	13,77	0,58	13,18	0,01
Sample Low 2	64,99	1,73	7,95	55,31	1362	227,3	339,7	794,9	15,06	0,53	14,51	0,01
Sample Low 3	58,39	1,99	8,62	47,77	794,1	162,7	150,2	481,2	15,24	0,54	14,69	0,01
Sample Med 1	37,27	1,14	3,08	33,06	880,1	199,9	159,5	520,8	15,84	0,48	15,34	0,01
Sample Med 2	40,11	1,30	3,53	35,27	759,6	170,8	93,29	495,5	13,59	0,51	13,07	0,01
Sample Med 3	41,83	1,35	5,32	35,17	741,2	169,6	120,6	451,1	13,97	0,46	13,50	0,01
Sample High 1	26,36	0,69	1,79	23,88	486,2	115,6	11,87	358,7	9,77	0,39	9,37	0,01
Sample High 2	28,45	0,70	1,55	26,20	618,1	143,7	0,14	474,2	11,40	0,58	10,81	0,01
Sample High 3	28,19	0,71	1,03	26,45	654,2	151,4	12,78	490,	13,27	0,44	12,82	0,01

Table 8. Determination of the particle number corresponding to each lipoprotein and its associated subcategories using the Optimized Protocol (BSA 40 mg/mL).

Optimized Protocol (BSA 40 mg/mL)	VLDL (nmol/L)				LDL (nmol/L)				HDL (μ mol/L)			
	P	L	M	S	P	L	M	S	P	L	M	S
Sample Low 1	59,77	2,30	5,39	52,09	587,2	123,5	24,44	439,3	11,88	0,49	11,38	0,01
Sample Low 2	63,82	1,68	8,06	54,08	1141	211,5	262,8	666,6	11,37	0,43	10,93	0,01
Sample Low 3	56,08	1,95	8,48	45,66	662,7	151,8	113,6	397,3	13,02	0,48	12,53	0,01
Sample Med 1	36,34	1,18	1,35	33,80	716,3	150,5	134,9	430,9	12,60	0,40	12,19	0,01
Sample Med 2	38,28	1,29	2,96	34,03	598,6	145,6	57,55	395,5	11,00	0,44	10,56	0,01
Sample Med 3	41,52	1,44	3,18	36,90	628,6	144,4	88,07	396,2	11,90	0,40	11,49	0,01
Sample High 1	26,97	0,69	1,22	25,06	471,7	122,7	0,12	348,9	9,63	0,42	9,20	0,01
Sample High 2	27,08	0,68	0,69	25,72	498,3	120,3	0,12	377,9	9,24	0,44	8,79	0,01
Sample High 3	27,33	0,68	0,69	25,95	579,5	138,7	0,14	440,7	11,62	0,41	11,20	0,01

Table 9. Determination of the mean size of each lipoprotein using the Standard Protocol.

Standard Protocol	VLDL (nm)	LDL (nm)	HDL (nm)
Sample Low 1	42,30	20,6	9,17
Sample Low 2	42,34	21,08	9,16
Sample Low 3	42,72	21,24	9,16
Sample Med 1	41,75	21,13	9,14
Sample Med 2	42,1	21,08	9,16
Sample Med 3	42,11	21,13	9,15
Sample High 1	41,67	20,88	9,17

Sample High 2	41,49	20,72	9,18
Sample High 3	41,49	20,7	9,15

Table 10. Determination of the mean size of each lipoprotein using the Optimized Protocol (BSA 30 mg/mL).

Optimized Protocol (BSA 30 mg/mL)	VLDL (nm)	LDL (nm)	HDL (nm)
Sample Low 1	42,74	20,93	9,17
Sample Low 2	42,32	20,99	9,15
Sample Low 3	42,68	21,09	9,15
Sample Med 1	42,07	21,26	9,14
Sample Med 2	42,16	21,02	9,16
Sample Med 3	42,48	21,20	9,15
Sample High 1	41,87	20,78	9,16
Sample High 2	41,72	20,64	9,19
Sample High 3	41,59	20,70	9,15

Table 11. Determination of the mean size of each lipoprotein using the Optimized Protocol (BSA 40 mg/mL).

Optimized Protocol (BSA 40 mg/mL)	VLDL (nm)	LDL (nm)	HDL (nm)
Sample Low 1	42,07	20,79	8,37
Sample Low 2	42,09	21,04	8,48
Sample Low 3	42,20	21,20	8,31
Sample Med 1	42,07	21,54	8,41
Sample Med 2	42,06	21,21	8,34
Sample Med 3	42,14	21,10	8,30
Sample High 1	42,23	20,80	8,34
Sample High 2	41,92	20,93	8,53
Sample High 3	41,90	21,02	8,33

9.2. ANNEX 2:

Table 12. Results of the univariate comparative analysis performed using the values obtained from the Liposcale software based on the spectra prior to Z-score normalization. The table shows the medians corresponding to each parameter analyzed for each of the protocols, with their standard deviations shown in parentheses. All statistically significant results (considering $p < 0.05$ as the threshold for significance) are highlighted in bold.

Univariate analysis of the protocols employed (previous Z-score)

	Optimized Protocol BSA 30	Optimized Protocol BSA 40	$p(<0.005)$	Standard Protocol 200	$p(<0.005)$	$p(<0.005)$	$p(<0.005)$
	N=9	N=9	Comparison between 30 vs 40	N=9	Comparison between 30 vs 200	Comparison between 40 vs 200	Comparison between 30 vs 40 vs 200
VLDL-C	16.1 [9.99;20.6]	13.4 [8.59;20.4]	0.508	25.0 [13.0;37.0]	0.171	0.102	0.188
IDL-C	4.90 [3.03;7.85]	3.93 [2.44;6.25]	0.564	12.4 [9.10;18.9]	0.012	0.003	0.005
LDL-C	78.6 [66.8;79.5]	63.7 [57.7;67.4]	0.102	114 [97.1;118]	0.024	0.002	0.003
HDL-C	42.8 [41.4;43.8]	35.1 [31.9;36.2]	0.005	57.4 [47.3;60.9]	0.005	<0.001	<0.001
VLDL-TG	51.7 [35.4;80.6]	50.4 [33.0;79.4]	0.508	83.3 [43.0;153]	0.102	0.102	0.148
IDL-TG	5.68 [3.59;6.74]	3.45 [2.91;5.45]	0.171	12.7 [10.1;16.3]	0.002	<0.001	<0.001
LDL-TG	6.46 [3.88;8.84]	4.88 [3.40;7.54]	0.566	15.9 [11.9;22.4]	0.009	0.003	0.005
HDL-TG	14.5 [12.1;16.7]	12.6 [10.7;14.0]	0.200	21.6 [18.1;25.7]	0.047	0.009	0.016
VLDL-P (nmol/L)	40.1 [28.4;56.6]	38.3 [27.3;56.1]	0.757	64.5 [33.2;118]	0.102	0.085	0.144
Large VLDL-P (nmol/L)	1.30 [0.71;1.73]	1.29 [0.69;1.68]	0.825	1.68 [0.98;2.44]	0.200	0.200	0.325
Medium VLDL-P (nmol/L)	3.53 [1.79;7.95]	2.96 [1.22;5.39]	0.310	5.96 [3.09;11.9]	0.200	0.070	0.137
Small VLDL-P (nmol/L)	35.2 [26.4;45.7]	34.0 [26.0;45.7]	0.895	56.9 [29.9;101]	0.058	0.070	0.097
LDL-P (nmol/L)	741 [654;794]	599 [579;663]	0.085	1169 [1020;1235]	0.012	0.001	0.001
Large LDL-P (nmol/L)	163 [146;171]	144 [123;150]	0.122	193 [157;201]	0.270	0.024	0.054
Medium LDL-P (nmol/L)	93.3 [12.8;150]	57.6 [0.14;114]	0.310	353 [246;391]	0.004	0.002	0.002
Small LDL-P (nmol/L)	481 [451;496]	397 [395;439]	0.024	617 [590;643]	0.019	0.004	0.002
HDL-P ($\mu\text{mol/L}$)	13.8 [13.3;15.1]	11.6 [11.0;11.9]	0.012	28.9 [26.3;32.5]	<0.001	<0.001	<0.001
Large HDL-P ($\mu\text{mol/L}$)	0.51 [0.46;0.54]	0.43 [0.41;0.44]	0.019	0.33 [0.31;0.40]	0.002	0.019	0.001
Medium HDL-P ($\mu\text{mol/L}$)	13.2 [12.8;14.5]	11.2 [10.6;11.5]	0.015	12.3 [11.9;13.0]	0.145	0.085	0.026
Small HDL-P ($\mu\text{mol/L}$)	0.01 [0.01;0.01]	0.01 [0.01;0.01]	0.019	16.7 [13.1;19.0]	<0.001	<0.001	<0.001
VLDL-Z (nm)	42.2 [41.9;42.5]	42.1 [41.7;42.3]	0.354	42.1 [42.1;42.1]	0.508	0.895	0.641
LDL-Z (nm)	21.0 [20.8;21.1]	21.1 [20.7;21.1]	0.965	21.0 [20.9;21.2]	0.354	0.453	0.620
HDL-Z (nm)	9.15 [9.15;9.16]	9.16 [9.15;9.17]	0.627	8.34 [8.33;8.41]	<0.001	<0.001	<0.001

Boxplots by Variable and Group

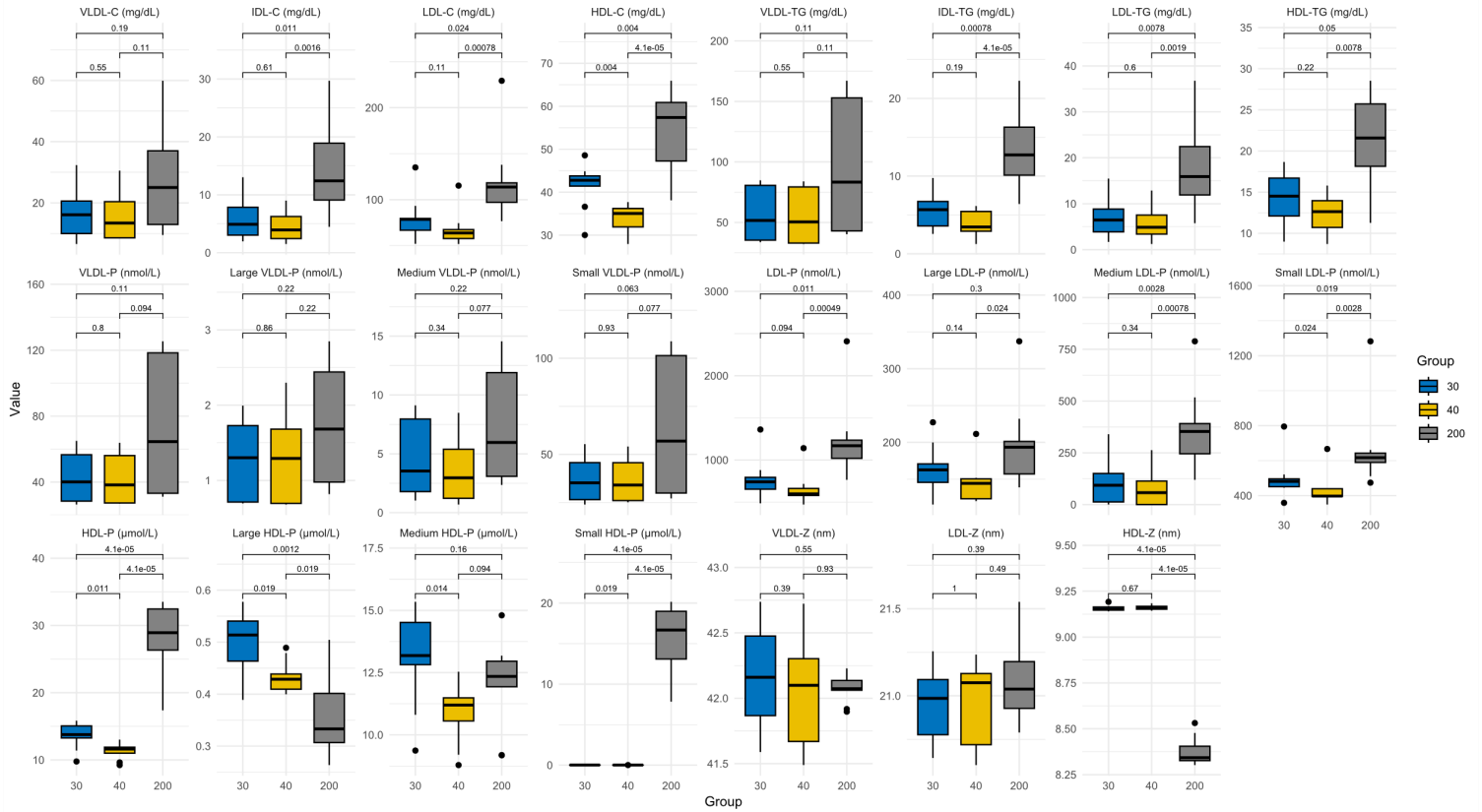


Figure 34. Boxplot representation of the data obtained through univariate analysis, showing the distribution of the values for each parameter and for each of the protocols analyzed (prior to Z-score normalization). In the figures, vertical black bars represent the standard deviations, and black dots indicate outliers, while the values above the brackets correspond to the p-values.

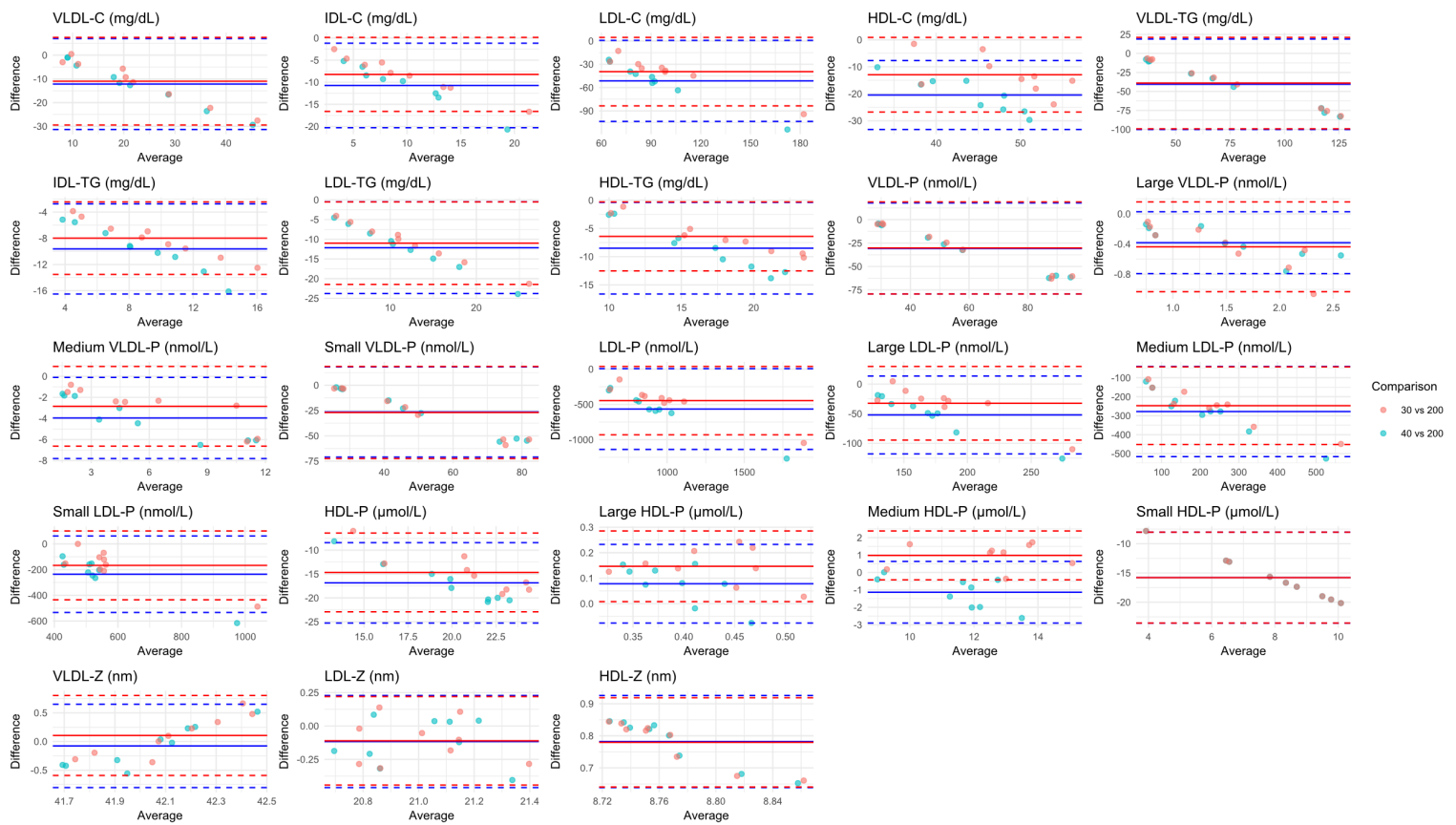


Figure 35. Graphical representation of the differences between protocols versus their mean for each of the parameters studied using the Bland-Altman method (prior to Z-score normalization). Each point represents an individual sample, while the solid lines indicate the mean difference between protocols, and the dashed lines represent the corresponding standard deviations.

9.3. ANNEX 3:

Table 13. Results of the univariate comparative analysis performed using the values obtained from the Liposcale software based on the spectra. The table shows the medians corresponding to each parameter analyzed for each of the protocols, with their standard deviations shown in parentheses. All statistically significant results (considering $p < 0.05$ as the threshold for significance) are highlighted in bold. Z-score normalization was applied to the values.

Univariate analysis of the protocols employed (Z-score)

	Optimized Protocol BSA 30	Optimized Protocol BSA 40	$p(<0.005)$	Standard Protocol 200	$p(<0.005)$	$p(<0.005)$	$p(<0.005)$
	N=9	N=9	Comparison between 30 vs 40	N=9	Comparison between 30 vs 200	Comparison between 40 vs 200	Comparison between 30 vs 40 vs 200
VLDL-C	26.1 [13.1;35.5]	22.5 [11.7;38.3]	0.895	25.0 [13.0;37.0]	0.825	0.965	0.979
IDL-C	13.5 [10.8;18.9]	13.7 [9.50;20.3]	1.000	13.4 [10.1;19.1]	0.916	0.916	0.998
LDL-C	117 [94.6;119]	110 [95.6;119]	0.895	114 [97.1;118]	0.965	0.965	0.995
HDL-C	56.7 [54.4;58.5]	57.5 [49.0;60.7]	0.825	57.4 [47.3;60.9]	0.825	0.965	0.967
VLDL-TG	84.4 [44.8;155]	85.3 [43.4;155]	0.895	83.3 [43.0;153]	0.895	0.965	0.993
IDL-TG	13.8 [9.32;16.1]	12.2 [10.6;18.0]	0.895	12.7 [10.1;16.3]	0.965	0.965	0.998
LDL-TG	16.8 [11.1;22.2]	15.5 [11.7;22.5]	0.965	15.9 [11.9;22.4]	0.965	0.965	0.998
HDL-TG	21.1 [16.6;25.3]	21.9 [16.7;25.5]	0.895	21.6 [18.1;25.7]	0.965	0.965	0.995
VLDL-P (nmol/L)	66.2 [34.4;111]	62.9 [33.4;111]	0.825	64.5 [33.2;118]	0.965	0.825	0.984
Large VLDL-P (nmol/L)	1.76 [0.86;2.41]	1.66 [0.89;2.17]	0.627	1.68 [0.98;2.44]	0.895	0.965	0.934
Medium VLDL-P (nmol/L)	5.79 [3.12;12.5]	6.56 [3.79;10.4]	0.757	5.96 [3.09;11.9]	0.965	0.757	0.937
Small VLDL-P (nmol/L)	59.2 [32.2;91.9]	54.4 [30.1;89.4]	0.895	56.9 [29.9;101]	0.965	0.895	0.993
LDL-P (nmol/L)	1157 [985;1261]	1083 [1036;1242]	0.965	1169 [1020;1235]	0.825	0.895	0.988
Large LDL-P (nmol/L)	193 [162;208]	195 [150;209]	0.965	193 [157;201]	0.825	0.895	0.977
Medium LDL-P (nmol/L)	328 [172;438]	311 [175;443]	0.691	353 [246;391]	0.895	0.965	0.967
Small LDL-P (nmol/L)	628 [568;657]	578 [573;686]	0.965	617 [590;643]	0.825	0.965	0.993
HDL-P (μmol/L)	28.8 [27.4;32.5]	29.3 [26.7;30.5]	0.965	28.9 [26.3;32.5]	0.895	0.895	0.988
Large HDL-P (μmol/L)	0.37 [0.31;0.40]	0.34 [0.30;0.37]	0.757	0.33 [0.31;0.40]	0.825	0.965	0.952
Medium HDL-P (μmol/L)	12.2 [11.8;13.5]	12.5 [11.5;12.9]	0.965	12.3 [11.9;13.0]	0.965	0.895	0.998
Small HDL-P (μmol/L)	16.5 [13.4;18.2]	15.2 [12.9;16.5]	0.757	16.7 [13.1;19.0]	0.895	0.627	0.898
VLDL-Z (nm)	42.1 [42.0;42.2]	42.1 [42.0;42.2]	0.895	42.1 [42.1;42.1]	0.895	0.825	0.998
LDL-Z (nm)	21.1 [20.9;21.2]	21.2 [20.8;21.2]	0.965	21.0 [20.9;21.2]	0.825	0.757	0.952
HDL-Z (nm)	8.35 [8.32;8.41]	8.37 [8.33;8.42]	0.895	8.34 [8.33;8.41]	0.825	0.965	0.995